

ไฮโดรคิซัลเฟอโรเซชันของน้ำมันที่ได้จากไพโรไลซิสยางรถยนต์ใช้แล้ว



วิทยานิพนธ์นี้เป็นส่วนหนึ่งของการศึกษาตามหลักสูตรปริญญาวิทยาศาสตรมหาบัณฑิต

สาขาวิชาปิโตรเคมีและวิทยาศาสตร์พอลิเมอร์

คณะวิทยาศาสตร์ จุฬาลงกรณ์มหาวิทยาลัย
บทคัดย่อและแฟ้มข้อมูลฉบับเต็มของวิทยานิพนธ์ตั้งแต่ปีการศึกษา 2554 ที่ให้บริการในคลังปัญญาจุฬาฯ (CUIR)
ปีการศึกษา 2556

เป็นแฟ้มข้อมูลของนิสิตเจ้าของวิทยานิพนธ์ ที่ส่งผ่านทางบัณฑิตวิทยาลัย
ลิขสิทธิ์ของจุฬาลงกรณ์มหาวิทยาลัย

The abstract and full text of theses from the academic year 2011 in Chulalongkorn University Intellectual Repository (CUIR) are the thesis authors' files submitted through the University Graduate School.

HYDRODESULFURIZATION OF OIL DERIVED FROM WASTE TIRE PYROLYSIS

Mr. Nut Jantaraksa



จุฬาลงกรณ์มหาวิทยาลัย
CHULALONGKORN UNIVERSITY

A Thesis Submitted in Partial Fulfillment of the Requirements
for the Degree of Master of Science Program in Petrochemistry and Polymer

Science

Faculty of Science

Chulalongkorn University

Academic Year 2013

Copyright of Chulalongkorn University

Thesis Title	HYDRODESULFURIZATION OF OIL DERIVED FROM WASTE TIRE PYROLYSIS
By	Mr. Nut Jantaraksa
Field of Study	Petrochemistry and Polymer Science
Thesis Advisor	Assistant Professor Dr. Napida Hinchiranan, Ph.D.
Thesis Co-Advisor	Professor Dr. Pattarapan Prasassarakich, Ph.D.

Accepted by the Faculty of Science, Chulalongkorn University in Partial
Fulfillment of the Requirements for the Master's Degree

.....Dean of the Faculty of Science
(Professor Dr. Supot Hannongbua, Ph.D.)

THESIS COMMITTEE

.....Chairman
(Professor Dr. Tharapong Vitidsant, Ph.D.)

.....Thesis Advisor
(Assistant Professor Dr. Napida Hinchiranan, Ph.D.)

.....Thesis Co-Advisor
(Professor Dr. Pattarapan Prasassarakich, Ph.D.)

.....Examiner
(Assistant Professor Dr. Varawut Tangpasuthadol, Ph.D.)

.....External Examiner
(Dr. Nikom Chawalitkijmongkol, Ph.D.)

ณัฐ จันทรักษา : ไฮโดรดีซัลเฟอไรเซชันของน้ำมันที่ได้จากไพโรไลซิสยางรถยนต์ใช้แล้ว.
(HYDRODESULFURIZATION OF OIL DERIVED FROM WASTE TIRE PYROLYSIS)
อ.ที่ปรึกษาวิทยานิพนธ์หลัก: ผศ. ดร. นพิตา ทิณชี่ระนันท์, อ.ที่ปรึกษาวิทยานิพนธ์
ร่วม: ศ. ดร. ภัทรพรรณ ประศาสน์สารกิจ, 87 หน้า.

ยางรถยนต์ใช้แล้วเป็นหนึ่งในทรัพยากรพลังงานทดแทนเนื่องจากประกอบด้วยไฮโดรคาร์บอนสายยาวซึ่งมีค่าความร้อนสูง อย่างไรก็ตามน้ำมันที่ได้จากการไพโรไลซิสยางรถยนต์ใช้แล้วไม่เหมาะที่จะนำมาใช้กับเครื่องยนต์โดยตรงเนื่องจากมันประกอบไปด้วยกำมะถันปริมาณสูง ดังนั้นจุดประสงค์ของงานวิจัยนี้ คือ ปรับปรุงคุณภาพของน้ำมันไพโรไลซิสจากยางรถยนต์ใช้แล้วด้วยการขจัดกำมะถันผ่านกระบวนการไฮโดรดีซัลเฟอไรเซชันโดยใช้ตัวเร่งปฏิกิริยาบนตัวรองรับแกมมาอะลูมินา (γ - Al_2O_3) 3 ชนิด คือ โมลิบดีนัม (Mo/γ - Al_2O_3) นิกเกิลโมลิบดีนัม (NiMo/γ - Al_2O_3) และโคบอลต์โมลิบดีนัม (CoMo/γ - Al_2O_3) ศึกษาผลของตัวแปรที่ใช้ในการไฮโดรดีซัลเฟอไรเซชัน ได้แก่ ปริมาณของตัวเร่งปฏิกิริยา (0-2 %โดยน้ำหนักของน้ำมันไพโรไลซิสจากยางรถยนต์ใช้แล้ว) ความดันไฮโดรเจนเริ่มต้น (10-50 บาร์) อุณหภูมิในการทำปฏิกิริยา (150-350 องศาเซลเซียส) และเวลาที่ใช้ในการทำปฏิกิริยา (5-60 นาที) พบว่า เมื่อใช้ปริมาณตัวเร่งปฏิกิริยาชนิดนิกเกิลโมลิบดีนัมบนตัวรองรับแกมมาอะลูมินา 2 %โดยน้ำหนักของน้ำมันไพโรไลซิสจากยางรถยนต์ใช้แล้ว ความดันไฮโดรเจนเริ่มต้น 20 บาร์ ที่อุณหภูมิ 250 องศาเซลเซียส ภายในเวลา 30 นาที ให้ประสิทธิภาพในการขจัดกำมะถันได้สูงสุดที่ 87.8% ปริมาณกำมะถันในน้ำมันไพโรไลซิสจากยางรถยนต์ใช้แล้วก่อนและหลังผ่านกระบวนการไฮโดรดีซัลเฟอไรเซชันถูกตรวจสอบด้วยแก๊สโครมาโทกราฟีชนิดเฟรมโฟโตเมตริกดีเทคเตอร์ พบว่ากระบวนการไฮโดรดีซัลเฟอไรเซชันมีประสิทธิภาพในการลดสารประกอบกำมะถันในน้ำมันไพโรไลซิสจากยางรถยนต์ใช้แล้ว โดยเฉพาะกลุ่มไทโอฟินและอนุพันธ์ของไทโอฟิน

จุฬาลงกรณ์มหาวิทยาลัย
CHULALONGKORN UNIVERSITY

สาขาวิชา ปีโตรเคมีและวิทยาศาสตร์พอลิเมอร์ ลายมือชื่อนิสิต

ปีการศึกษา 2556

ลายมือชื่อ อ.ที่ปรึกษาวิทยานิพนธ์หลัก

ลายมือชื่อ อ.ที่ปรึกษาวิทยานิพนธ์ร่วม

5372239223 : MAJOR PETROCHEMISTRY AND POLYMER SCIENCE

KEYWORDS: HYDRODESULFURIZATION / WASTE TIRE / PYROLYSIS / CATALYST

NUT JANTARAKSA: HYDRODESULFURIZATION OF OIL DERIVED FROM WASTE TIRE PYROLYSIS. ADVISOR: ASST. PROF. DR. NAPIDA HINCHIRANAN, Ph.D., CO-ADVISOR: PROF. DR. PATTARAPAN PRASASSARAKICH, Ph.D., 87 pp.

The waste tire is one of alternative energy sources due to its long hydrocarbon chains with high heating value. However, the oil derived from waste tire pyrolysis is not suitably used in any combustion engines since it contains a huge volume of sulfur compounds. Therefore, the aim of this research was to improve the waste tire pyrolysis oil via hydrodesulfurization catalyzed by using 3 types of catalysts supported on γ -alumina: molybdenum ($\text{Mo}/\gamma\text{-Al}_2\text{O}_3$), nickel-molybdenum ($\text{NiMo}/\gamma\text{-Al}_2\text{O}_3$) and cobalt-molybdenum ($\text{CoMo}/\gamma\text{-Al}_2\text{O}_3$). The catalyst prepared by successive incipient wetness impregnation method. The effects of catalyst loading (0-2 wt% based on the amount of waste tire pyrolysis oil), initial hydrogen pressure (10-50 bar), reaction temperature (150-350 °C), and reaction time (5-60 min) on the %sulfur removal were investigated. The maximum %sulfur removal at 87.8% was achieved when the reaction was carried out at 250 °C for 30 min by using 2 wt% of catalyst loading and 20 bar of initial hydrogen pressure. The amount of sulfurous compounds in the waste tire pyrolysis oil was determined by using gas chromatography equipped with a flame photometric detector (GC-FPD). The results indicated that hydrodesulfurization of waste tire pyrolysis oil was effective to reduce the sulfurous compounds; especially, thiophene and its derivatives.

จุฬาลงกรณ์มหาวิทยาลัย
CHULALONGKORN UNIVERSITY

Field of Study: Petrochemistry and
Polymer Science

Academic Year: 2013

Student's Signature

Advisor's Signature

Co-Advisor's Signature

ACKNOWLEDGEMENTS

The author wishes to express greatest gratitude to his advisor, Assistant Professor Dr. Napida Hinchiranan, for her advice, assistance and generous encouragement throughout the course of this research. In addition, the author wishes to express deep appreciation to Professor Tharapong Vitidsant, Professor Pattarapan Prasassanakich, Assistant Professor Varawut Tangpasuthadol and Dr. Nikom Chawalitkijmongkol for serving as the chairman, co-advisor and members of his thesis committee, respectively, and provide their valuable suggestions and comments.

Appreciation is also extended to Program of Petrochemistry and Polymer Science and the Department of chemical Technology, Faculty of Science, Chulalongkorn University for granting financial support to fulfill this study and provision of experimental facilities.

The author is thankful to The Energy Policy and Planning Office for financial support throughout this research. The author wishes to express deep appreciation to The Union Commercial Development Co., Ltd. (Samutprakarn, Thailand) for support the waste tire powder. Finally, the author is very appreciated to his family and his best friends for their assistance and encouragement throughout his entire education.



จุฬาลงกรณ์มหาวิทยาลัย
CHULALONGKORN UNIVERSITY

CONTENTS

	Page
THAI ABSTRACT	iv
ENGLISH ABSTRACT	v
ACKNOWLEDGEMENTS	vi
CONTENTS	vii
LIST OF TABLES	xi
LIST OF FIGURES	xii
CHAPTER I	1
INTRODUCTION	1
1.1 The Statement of Problem	1
1.2 Objectives of the Research Work	3
1.3 The Scope of This Research Work	3
CHAPTER II	5
THEORY AND LITERATURE REVIEWS	5
2.1 Tire	5
2.2 Vulcanization	7
2.3 Sulfur Vulcanization	8
2.4 Waste Tire	10
2.5 Pyrolysis	12
2.6 Pyrolysis of Waste Tire	13
2.7 Sulfur Compounds in Waste Tire Pyrolysis Oil Compared to Petroleum Products	15
2.8 Current Desulfurization Technologies	18
2.8.1 Hydrodesulfurization	18
2.8.2 Oxidative Desulfurization	20
2.8.3 Biodesulfurization	21
2.8.4 Adsorptive Desulfurization	22
2.8.5 Photocatalytic Desulfurization	22

	Page
2.9 Literature Reviews.....	23
CHAPTER III.....	26
EXPERIMENT AND CHARACTERIZATION	26
3.1 Materials	26
3.2 Experimental Procedures	27
3.2.1 Pyrolysis Process	27
3.2.2 Catalyst Preparation	27
3.2.3 Hydrodesulfurization of Waste Tire Pyrolysis Oil	28
3.3 Analytical Methods.....	28
3.3.1 Characterization of Waste Tire Powder and its Pyrolysis Oil	28
3.3.2 Catalyst Characterization.....	29
3.3.2.1 BET Surface Area.....	29
3.3.2.2 Scanning Electron Microscopy/Energy Dispersive X-ray Spectroscopy (SEM/EDX).....	29
3.3.2.3 X-Ray Diffraction (XRD)	29
3.3.2.4 Temperature Programmed Reduction (TPR)	29
3.3.2.5 Temperature Programmed Desorption (TPD)	30
3.3.3 Type and Content of Sulfurous Compounds in the Waste Tire Pyrolysis Oil.....	30
3.3.4 Quality of Waste Tire Pyrolysis Oil after Hydrodesulfurization	31
3.3.4.1 Gas Chromatography Simulated Distillation (GC-SIMDIS).....	31
3.3.4.2 Gas Chromatography/Mass Spectroscopy (GC/MS).....	31
3.3.4.3 Viscosity, Copper Strip Corrosion, Heating Value and Iodide Value	32
CHAPTER IV	33
RESULT AND DISCUSSION.....	33
4.1 Characterization of Waste Tire Powder	33
4.2 Products Derived from Waste Tire Pyrolysis	35

	Page
4.3 Catalysts Characterization	36
4.3.1 Scanning Electron Microscopy/Energy Dispersive X-ray Spectroscopy (SEM/EDX).....	37
4.3.2 BET Surface Area	40
4.3.3 X-Ray Diffraction (XRD).....	42
4.3.4 Temperature Programmed Reduction (TPR)	44
4.3.5 Temperature Programmed Desorption (TPD)	47
4.4 Characterization of Sulfurous Compounds Containing in the Waste Tire Pyrolysis Oil	49
4.5 Hydrodesulfurization of Waste Tire Pyrolysis Oil	51
4.5.1 Effect of Catalyst Types and Concentration	51
4.5.2 Effect of Initial Hydrogen Pressure	54
4.5.3 Effect of Reaction Temperature	56
4.5.4 Effect of Reaction Time.....	57
4.6 Quality of Waste Tire Pyrolysis Oil after Hydrodesulfurization	58
4.6.1 Appearance of Waste Tire Pyrolysis Oil after Hydrodesulfurization.....	58
4.6.2 Gas Chromatography Simulated Distillation (GC-SIMDIS).....	59
4.6.3 Gas Chromatography/Mass Spectroscopy (GC/MS).....	61
4.6.4 Viscosity, Copper Strip Corrosion, Heating Value and Iodine Value.....	63
CHAPTER V	66
CONCLUSIONS	66
5.1 Conclusions.....	66
5.1.1 Characterization of Waste Tire and Its Pyrolysis Products	66
5.1.2 Catalysts Characterization.....	67
5.1.3 Hydrodesulfurization of Waste Tire Pyrolysis Oil	67
5.1.4 Quality of Waste Tire Pyrolysis Oil after Hydrodesulfurization	68
5.2 Recommendations.....	68
REFERENCES	69

	Page
APPENDIX A.....	77
CALCULATION OF PRODUCT YIELDS.....	77
APPENDIX B.....	79
CALCULATION OF GROSS CALORIFIC HEATING VALUE.....	79
APPENDIX C.....	81
CALCULATION OF %SULFUR REMOVAL.....	81
APPENDIX D.....	83
DATA OF SULFUR REMOVAL EFFICIENCY.....	83
VITA.....	87

LIST OF TABLES

	Page
Table 1.1 Standards for Transportation Fuels in the European Union	2
Table 2.1 Basic Composition of Tire Rubber	6
Table 2.2 Vulcanizate Structures and Properties.....	9
Table 2.3 Typical Composition of the Waste Tire Feedstock.....	11
Table 2.4 Example of Some Sulfur Compounds in Crude Oil	16
Table 2.5 Characteristics of Some Typical Crude Oils	17
Table 4.1 Composition of Waste Tire Powder Feedstock.....	33
Table 4.2 Yields of Waste Tire Pyrolysis Products at 400 °C.....	35
Table 4.3 Ultimate Analysis of Condensed Oil Fraction and Heating Value.....	36
Table 4.4 Elemental Analysis of Each Studied Catalysts	39
Table 4.5 BET Surface Area, Total Pore Volume and Average Pore Diameter..	42
Table 4.6 %Mass of the Waste Tire Pyrolysis Oil before and after Hydrodesulfurization.....	60
Table 4.7 Tentative GC/MS Characterization of Waste Tire Pyrolysis Oil	63
Table 4.8 Viscosity, Copper Strip Corrosion, Heating Value and Iodine Value of Oils	64

LIST OF FIGURES

	Page
Figure 2.1 Chemical Structures of Natural Rubber and Synthetic Rubbers.....	5
Figure 2.2 Properties as a Function of the Extent of Crosslinking.....	7
Figure 2.3 Structural Features of a Sulfur-Vulcanized Natural Rubber Network.....	8
Figure 2.4 GC-FPD Chromatogram of Waste Tire Pyrolysis Oil.....	18
Figure 2.5 Diagram of a Hydrodesulfurization Cycle of Thiophene.....	19
Figure 2.6 Simplified Network for Oxidative Desulfurization of Dibenzothiophene	20
Figure 2.7 Simplified Sulfur-Specific Biodesulfurization of Dibenzothiophene.....	21
Figure 3.1 Schematic Diagram of Pyrolysis Process.....	27
Figure 4.1 TGA Thermogram of Waste tire powder.....	34
Figure 4.2 Schematic Diagram of Catalyst Preparation.....	37
Figure 4.3 SEM/EDX Characterization: (a) Mo Mapping of Mo/ γ -Al ₂ O ₃ Catalyst, (b) Mo Mapping of NiMo/ γ -Al ₂ O ₃ Catalyst, (c) Mo Mapping of CoMo/ γ -Al ₂ O ₃ Catalyst, (d) Ni Mapping of NiMo/ γ -Al ₂ O ₃ Catalyst and (e) Co Mapping of CoMo/ γ -Al ₂ O ₃ Catalyst.....	38
Figure 4.4 Adsorption - Desorption Isotherm of (a) Mo/ γ -Al ₂ O ₃ (b) NiMo/ γ -Al ₂ O ₃ and (c) CoMo/ γ -Al ₂ O ₃ Catalysts.....	41
Figure 4.5 XRD patterns of (a) Mo/ γ -Al ₂ O ₃ (b) NiMo/ γ -Al ₂ O ₃ and (c) CoMo/ γ -Al ₂ O ₃ Catalysts.....	43
Figure 4.6 TPR Profiles of (a) Mo/ γ -Al ₂ O ₃ (b) NiMo/ γ -Al ₂ O ₃ and (c) CoMo/ γ -Al ₂ O ₃ Catalysts.....	45

Figure 4.7 TPD Profiles of (a) Mo/ γ -Al ₂ O ₃ (b) NiMo/ γ -Al ₂ O ₃ and (c) CoMo/ γ -Al ₂ O ₃ Catalysts	48
Figure 4.8 Waste Tire Pyrolysis Oil before Hydrodesulfurization	49
Figure 4.9 GC - FPD Chromatograms of (a) Standard of Sulfurous Compounds (Thiophene, Benzothiophene and Dibenzothiophene) and (b) Waste Tire Pyrolysis Oil.....	50
Figure 4.10 Effect of Catalyst Concentration on %Sulfur Removal in the Waste Tire Pyrolysis Oil via Hydrodesulfurization using Mo/ γ -Al ₂ O ₃ , CoMo/ γ -Al ₂ O ₃ and NiMo/Al ₂ O ₃ Catalysts (P _{H2} = 20 bar, T = 250 °C for 30 min)	52
Figure 4.11 GC-FPD Chromatograms of Waste Tire Pyrolysis Oil after Hydrodesulfurization using (a) Mo/ γ -Al ₂ O ₃ (50.4% sulfur removal), (b) NiMo/ γ -Al ₂ O ₃ (87.8% sulfur removal) and (c) CoMo/ γ -Al ₂ O ₃ (78.8% sulfur removal) Catalysts.....	53
Figure 4.12 Effect of Initial Hydrogen Pressure on %Sulfur Removal in the Waste Tire Pyrolysis Oil via Hydrodesulfurization using Mo/ γ -Al ₂ O ₃ , CoMo/ γ -Al ₂ O ₃ and NiMo/ γ -Al ₂ O ₃ Catalysts (Catalyst Concentration = 0.5 wt%, T = 250 °C for 30 min).	55
Figure 4.13 Effect of Reaction Temperature on %Sulfur Removal in the Waste Tire Pyrolysis Oil via Hydrodesulfurization using Mo/ γ -Al ₂ O ₃ , CoMo/ γ -Al ₂ O ₃ and NiMo/ γ -Al ₂ O ₃ Catalysts (Catalyst Concentration = 0.5 wt%, P _{H2} = 20 bar for 30 min)	56
Figure 4.14 Effect of Reaction Time on %Sulfur Removal in the Waste Tire Pyrolysis Oil via Hydrodesulfurization using Mo/ γ -Al ₂ O ₃ , CoMo/ γ -Al ₂ O ₃ and NiMo/ γ -Al ₂ O ₃ Catalysts (Catalyst Concentration = 0.5 wt%, P _{H2} = 20 bar, T = 250 °C).....	58
Figure 4.15 Waste Tire Pyrolysis Oil after Hydrodesulfurization.	59

Figure 4.16 GC-SIMDIS chromatograms of Diesel, Gasoline, Waste Tire Pyrolysis Oil before and after Hydrodesulfurization (87.8% sulfur removal)..... 60

Figure 4.17 GC/MS Chromatograms of Waste Tire Pyrolysis Oil (a) before and (b) after Hydrodesulfurization. 62



CHAPTER I

INTRODUCTION

1.1 The Statement of Problem

The quantity of waste tire is annually increased due to the growth of population and higher demands for personal transportation including the enhancement of industrial sectors. Since the waste tire is not a kind of biodegradable materials, it promotes the pollution during its combustion by releasing the sulfur dioxide (SO₂) and polycyclic aromatic hydrocarbons (PAHs) resulting from the vulcanizing agents and elastomers, respectively. However, the waste tire has been considered as one of alternative energy sources due to its higher heating value (39.1 MJ/kg) (Cao et al., 2009) than that of biomass such as rice husk (13-16 MJ/kg) (Natarajan et al., 1998) or palm (18-20 MJ/kg) (Vijaya et al., 2004). Thus, the technology used for improvement of the quality of the alternative energy generated from the waste tire for the environmental aspect should be investigated.

The one of appropriate methods to manage the waste tire is to transform it as the source of alternative energy by using the thermal decomposition process without the participation of oxygen or called as "pyrolysis". It is irreversible and involves the simultaneous change of chemical composition and physical phases. Products derived from pyrolysis can be categorized as three types: oil, char and gases (Juma et al., 2006). The pyrolysis char can be used as an activated carbon or reinforcing filler in the rubber industry. Whereas, the liquid product containing various organic compounds having 5-20 carbons with aromatics proportion may be used as fuels or petroleum refinery feedstock. However, the waste tire pyrolysis oil having high sulfur content (1.0-1.4% wt%) generated from the vulcanizing agents used for tire production (Laresgoiti et al., 2004) is limited to be directly applied for the combustion engines. These sulfur compounds such as thiols, sulfides, thiophenes, benzothiophenes, dibenzothiophenes and their derivatives in the waste tire pyrolysis oil induce undesired properties such as corrosiveness with highly toxic SO₂ gas generated during combustion. Thus, it was necessary to seek the process for removal of sulfur compounds from waste tire pyrolysis oil before using or blending with the commercial fossil liquid fuels.

Table 1.1 presents the specifications for gasoline and diesel in Europe (Walsh, 2006). These new regulations are also implemented in the United States, Taiwan, and Japan including other parts of Asia. This indicates that technology and unit operations in modern petroleum refineries have to be developed to meet very low level of sulfur content in the transportation liquid fuels (≤ 10 ppm). Traditionally, the removal of sulfur compounds from petroleum-derived feedstocks has been achieved via hydrodesulfurization (HDS) to convert sulfur substances as hydrogen sulfides (H_2S). This reaction is performed on the surface of the catalyst under high hydrogen pressure (30-130 atm) and temperature (300-400 °C). Conventional catalysts used for hydrodesulfurization are in sulfided form of cobalt-molybdenum (CoMo) or nickel-molybdenum (NiMo) supported on alumina (Al_2O_3). In the previous literatures (Moses et al., 2007, Wang et al., 2008, Alibouria et al., 2009 and Yoosuk et al., 2008), the removal of sulfur compounds via hydrodesulfurization has been reported by using models of sulfurous substances such as thiophene, benzothiophene, dibenzothiophene and 4,6 dimethyldibenzothiophene.

Table 1.1 Standards for Transportation Fuels in the European Union (Walsh, 2006)

	European Commission			
	1996 (Euro 2)	2000 (Euro 3)	2005 (Euro 4)	Current standard 2009 (Euro 5)
Gasoline				
Benzene (%)	None	1	1	None
Aromatics (%)	None	42	35	None
Sulfur (ppm) *	500	150	50	10
Diesel				
Cetane min.	48	51	51	None
PAHs (%)	None	11	11	None
Sulfur (ppm)	500	350	50	10

*ppm = Parts per million

Unlike the conventional fossil liquid fuels, the sulfur compounds found in the waste tire pyrolysis oil are more complicated. Thus, this research focused on the reduction of sulfur content in the waste tire pyrolysis oil via hydrodesulfurization catalyzed by using molybdenum supported on γ -alumina ($\text{Mo}/\gamma\text{-Al}_2\text{O}_3$), nickel-molybdenum supported on γ -alumina ($\text{NiMo}/\gamma\text{-Al}_2\text{O}_3$) and cobalt-molybdenum supported on γ -alumina ($\text{CoMo}/\gamma\text{-Al}_2\text{O}_3$). The effects of studied parameters: catalyst concentration, initial hydrogen pressure, reaction temperature, reaction time on the %sulfur removal were investigated.

1.2 Objectives of the Research Work

The objectives of this research were stated as followed:

1. To study the hydrodesulfurization of the pyrolysis oil derived from waste tire.
2. To investigate the effect of reaction parameters: catalyst concentration, initial hydrogen pressure, reaction temperature, reaction time to achieve high %sulfur removal.

1.3 The Scope of This Research Work

The details of experimental procedure for this research were briefly presented as followed:

1. Survey previous literatures related to this work.
2. Prepare materials, design and construct the reactor for hydrodesulfurization.
3. Characterize the waste tire powder ($\text{Ø} = 250 \mu\text{m}$): proximate analysis, ultimate analysis, heating value and sulfur content.
4. Prepare the pyrolysis oil from pyrolysis of waste tire powder in a fixed bed reactor at 400°C under nitrogen atmosphere with a flow rate of 0.1 L/min for 15 min and then analyze its gross calorific value and total sulfur content using sulfur analyzer and gas chromatography equipped with a flame photometric detector (GC-FPD).

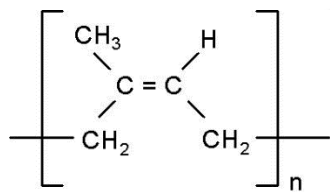
5. Investigate the effect of reaction parameters for the hydrodesulfurization of waste tire pyrolysis oil on the %sulfur removal as follow:
 - Type of catalyst: Mo/ γ -Al₂O₃, NiMo/ γ -Al₂O₃, CoMo/ γ -Al₂O₃
 - Catalyst concentration: 0-2 wt%
 - Initial hydrogen pressure: 10-50 bar
 - Reaction temperature: 150-350 °C
 - Reaction time: 5-60 min
6. Analyze type and content of remaining sulfurous compounds in the waste tire pyrolysis oil by using GC-FPD after hydrodesulfurization.
7. Investigate the quality of the waste tire pyrolysis oil after hydrodesulfurization:
 - Heating value
 - Viscosity
 - Copper strip corrosion
 - Iodine value
8. Summarize the results.

CHAPTER II

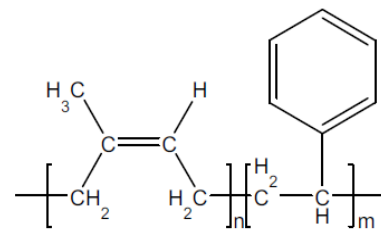
THEORY AND LITERATURE REVIEWS

2.1 Tire

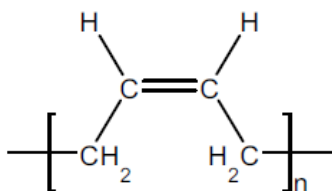
A tire is a strong and flexible rubber attached to the rim of a wheel. Tires provide a gripping surface for traction and serve as a cushion for the wheels of a moving vehicle. Tires are used in automobiles, trucks, buses, aircraft landing gear, tractors and other farm equipment, industrial vehicles such as forklifts and common conveyances such as baby carriages, shopping carts, wheel chairs, bicycles, and motorcycles (Rodgers and Waddell, 2013). Natural rubber is mainly used in manufacturing tires in cooperation with synthetic rubbers. In order to develop the proper characteristics of strength, resiliency and wear-resistance, the rubbers must be treated with a variety of chemicals and then heated. The natural rubber is generated from the Hevea tree, while the synthetic rubbers are generally derived from petroleum-based products. Figure 2.1 shows chemical structures of natural rubber and synthetic rubber normally used for tire production.



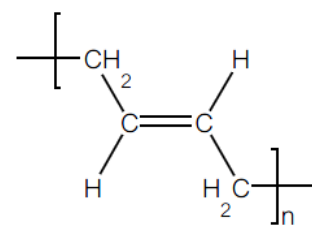
a) Natural rubber



b) Styrene butadiene rubber



c) *Cis*-1,4-butadiene



d) *Trans*-1,4-butadiene

Figure 2.1 Chemical Structures of Natural Rubber and Synthetic Rubbers.

Tires are consisted of rubbers (60-65 wt%), carbon black (25-35 wt%) and other chemicals such as accelerators and activators (Martinez et al., 2013). Carbon black, a fine and soft powder produced by the combustion of crude oil or natural gas in the presence of the limited amount of oxygen, is used as a reinforcing filler to strengthen the rubbers and to increase their abrasion resistance. In contrast, the addition of an extender oil decreases the hardness of rubbers resulting in the improvement of workability (Amari et al., 1999). The chemical process for converting rubbers into more durable materials is vulcanization. This process can improve the physical properties of natural or synthetic rubbers. The finished rubbers have higher tensile strength with increasing the swelling resistance and abrasion property. Moreover, the vulcanized rubbers are elastic over a greater range of temperatures. The vulcanization of rubbers normally requires the assistance of accelerators and activators such as zinc oxide and stearic acid including antidegradants, which are used to prevent degradation of the finished products during vulcanization or operations. A typical composition for tire is shown in Table 2.1.

Table 2.1 Basic Composition of Tire Rubber (Pehlken and Essadiqi, 2005)

Composition of tire	Example of main compounding ingredients	wt%
Rubbers	Natural rubber, synthetic rubbers	51.0
Reinforcing agents	Carbon black, silica	25.0
Softeners	Petroleum process oil, petroleum synthetic resin, etc.	19.5
Vulcanizing accelerators	Thiazole accelerators, sulfenic amide accelerator	1.5
Vulcanizing agents	Sulfur, organic vulcanizers	1.0
Vulcanizing accelerator aids	Zinc oxide, stearic acid	0.5
Antioxidants	Amine antioxidants, phenol antioxidants, wax	} 1.5
Fillers	Calcium carbonate, clay	

2.2 Vulcanization

Vulcanization is a process generally applied to rubbery or elastomeric materials to increase their dynamically mechanical strength and the retractile force with reducing the amount of permanent deformation remaining after removal of the deforming force. Thus, vulcanization increases elasticity with decreasing plasticity (Rattanasupa, 2007). Normally, vulcanization is used to convert rubber molecules into a network by formation of crosslinks between the polymer chains. Vulcanization is normally accomplished by applying heat for a specified time at the desired level. The most common methods for vulcanization are carried out in a compression molds and heated by contacting with steam-heated plates or electrical heater maintained at the desired temperature. Major effects of crosslinking on use-related properties are shown in Figure 2.2. Modulus and hardness are increased with increasing the crosslinking level. In contrast, the hysteresis is reduced with increasing the crosslink formation. Tear strength, fatigue life, and toughness of the vulcanized rubbers are related to the breaking energy. Values of these properties increase with small amounts of crosslinking, but they are reduced by further crosslink formation (Orza, 2008).

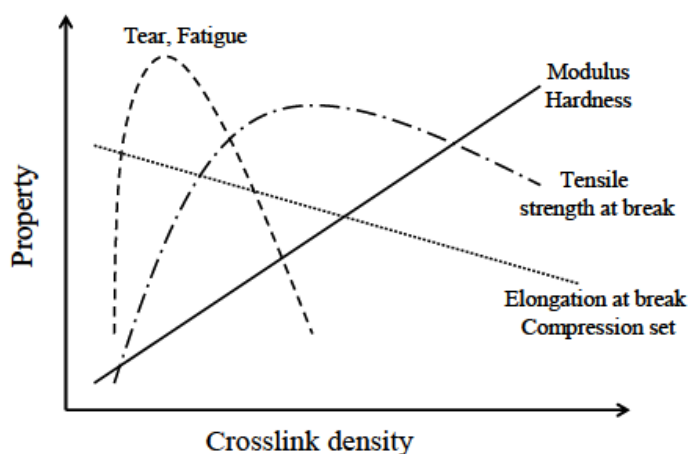


Figure 2.2 Properties as a Function of the Extent of Crosslinking (Orza, 2008).

2.3 Sulfur Vulcanization

Vulcanizing agents are necessary for the crosslink formation. Most of vulcanizing agents is sulfur or peroxides. Occasionally, other special vulcanizing agents or high energy radiation may be applied. The first and by far the most important crosslinking agent is sulfur used for curing unsaturated rubbers containing double bonds with allylic hydrogens such as natural rubber (NR), styrene butadiene rubber (SBR) and butadiene rubber (BR) because of its versatility and reasonable price (Hamed, 1992). The advantage of this system relates to its efficiency to promote the fast crosslink formation between rubber macromolecules in the presence of accelerators and activators. The crosslink may be a group of sulfur atoms in a short chains, a single sulfur atom, carbon-to-carbon bonds, polyvalent organic radicals, ionic clusters, or polyvalent metal ions. Sulfur exists in the elemental state as an eight-membered ring (S_8) (Hertz, 1984). The ultimate properties in terms of hardness and elasticity are depended on the course of the vulcanization.

Figure 2.3 shows the sulfur linkages generated during vulcanization in several forms: monosulfide, disulfide or polysulfide (Figure 2.3a), pendant sulfides terminated by moiety X derived from the used accelerator (Figure 2.3b), or cyclic monosulfides or disulfides (Figure 2.3c) (Niyogi, 2007). The number of sulfur atoms in the crosslink strongly influences the physical properties of the final rubber products. The short crosslinks give the rubber with better heat resistance. Whereas, the crosslinks with higher number of sulfur atoms give the rubber with good dynamic properties with poor heat resistance.

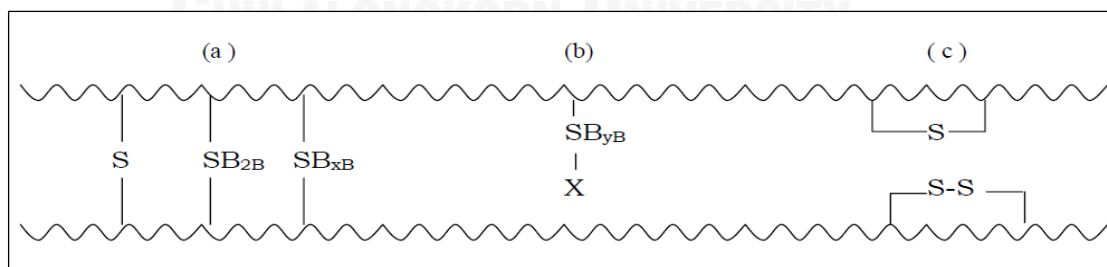


Figure 2.3 Structural Features of a Sulfur-Vulcanized Natural Rubber Network (Niyogi, 2007).

Sulfur vulcanization can be categorized as 3 system: conventional vulcanization (CV), efficient vulcanization (EV) and semi-efficient vulcanization (SEV). The CV system has sulfur content about 2.0-3.5 parts per hundred of rubber (phr). It provides higher amounts of polysulfide and disulfide crosslinks with higher proportions of sulfidic and non-sulfidic modifications as a result of high flex fatigue resistance and dynamic properties. However, the obtained rubber products generally has worse thermal and reversion resistance. The EV system is the lowest sulfur content (0.4-0.8 phr) and a correspondingly high level of accelerator or sulfurless curing employed in vulcanization process requiring the extremely high heat and reversion resistance. For the optimum levels of mechanical and dynamic properties of vulcanizates with intermediate heat, reversion, flex and dynamic properties, the SEV system with an intermediate contents of accelerator and sulfur (1-1.7 phr) are employed (Datta, 2002). The vulcanizate structures and properties for CV, EV and SEV systems are shown in Table 2.2.

Table 2.2 Vulcanizate Structures and Properties (Datta, 2002)

	Systems		
	CV	SEV	EV
Poly- and disulfidic crosslinks (%)	95	50	20
Monosulfidic crosslinks (%)	5	50	80
Cyclic sulfidic (conc.)	High	Medium	Low
Non-sulfidic (conc.)	High	Medium	Low
Reversion resistance	Low	Medium	High
Heat aging resistance	Low	Medium	High
Fatigue resistance	High	Medium	Low
Heat build up	High	Medium	Low
Tear resistance	High	Medium	Low
Compression set (%)	High	Medium	Low

2.4 Waste Tire

With annually increasing a number of motor vehicles in the world, there is a rapid increase in the amount of waste tires. Approximately, 5×10^6 tons/year of waste tire generated in the world were produced in Europe as 2×10^6 tons, in North America as 2.5×10^6 tons and in Japan 0.5×10^6 tons (Galvagno et al., 2002). The huge quantities of waste tires lead serious environmental issues regarding their disposal. The main reason for this problem is that waste tires are not biodegradable and they have to spend > 100 years to be degraded if they are not properly managed. There are different methods to treat the waste tire. The common process to extend the lifespan of a worn tire is retreaded or recapped or remolded. Land filling is one of the most tire disposal to tackle the waste tire problem. However, many countries have proposed to ban this method since metals and contaminants from tire pieces can be leached into the natural water resource possibly inducing the liver lesion (Bhatt and Patel, 2012). Recycling waste tire to raw rubber materials seems practicable. However, the more profitable process for energy and chemicals recovery from waste tire are more attractive than the conventional recycling process of tire.

Pyrolysis, incineration, co-combustion, tire derived fuel (TDF), liquefaction and gasification can recover energy and/or valuable chemicals from the treatment of waste tires. However, the incineration and TDF may involve the emission of hazardous pollutants, which are extremely harmful to human health and natural environment. The fumes emitted are consisted of with many toxic chemicals and organic compounds such as benzene, lead, polycyclic aromatic hydrocarbons (PAHs): benzo(a)pyrene. Additionally, the chlorine content in tires can promote the production of dioxins and furans during combustion (Bhatt and Patel, 2012). Moreover, the amount of sulfur components in the waste tire is normally larger than 1 wt%. Thus, the incineration and TDF should not be suitable method to directly recover energy from the waste tire.

At the present time, there is no perfect approach to recycle waste tires. As a result, illegal dumping or open burning can be seen everywhere. The air pollutants generated during tire combustion is the dense black smoke, which impairs visibility and soils painted surfaces. Toxic gas emissions include polyaromatic hydrocarbons, CO, SO₂, and NO₂. The heat from tire combustion also causes some of the rubber to break down into an oily material, which can contaminate the surface and groundwater. Incorrect methods of waste tires disposal can damage environment and public

health. Moreover, the curve shape of waste tire can collect rainwater resulting to create the habitat for rodents and mosquitoes (Islam et al., 2013). However, the waste tire are used for several applications in civil engineering project, alternative energy sources, recycled rubber goods, rubber-modified asphalt, recycled into cut/stamped/punched products, agricultural activities.

The compositions of waste tire investigated by using ultimate analysis and proximate analysis are shown in Table 2.3. According to high volatiles and fixed carbon contents, the waste tire has high heating value as 40 MJ/kg (Williams and Bottrill, 1995). Thus, the waste tires are interesting materials for using as an alternative energy resource.

Table 2.3 Typical Composition of the Waste Tire Feedstock (Williams and Bottrill, 1995)

Analysis	Values
<u>Proximate analysis (wt%)</u>	
● Volatiles	66.5
● Fixed carbon	30.3
● Ash	2.4
● Moisture	0.8
<u>Ultimate analysis (wt%)</u>	
● Carbon	85.9
● Hydrogen	8.0
● Nitrogen	0.4
● Sulfur	1.0
● Oxygen	2.3
Heating value (MJ/kg)	40

2.5 Pyrolysis (Wang and Qing, 2011)

Due to the waste tire having a high heating value generated from long hydrocarbon chains of natural rubber and synthetic rubbers, the waste tire has high potential to replace the conventional fossil fuels. Generally, the process for transformation of the waste tire as the source of alternative energy is pyrolysis, which is a kind of thermal decomposition process to degrade the solid materials in the absence of oxygen. The feedstock and processing conditions influence on the type of pyrolysis products and their yields. Pyrolysis temperature, pressure, heating rate, retention time and material size etc. are the main influence factors. Typically, the process is performed either in the presence of a flow of inert gas or under vacuum. For the pyrolysis of waste tire, the rubbers and other organic compounds in the waste tire are decomposed and are converted as oil and gas. The pyrolysis residue consists of the recovered carbon black filler, inorganic substances and several carbonaceous materials. According to the process temperature, the pyrolysis steps can be described as followed:

- 1) 100 °C to 120 °C: Dry and separate water with no decomposed substances;
- 2) < 250 °C: Break down the structure of materials and release water and CO₂;
- 3) > 250 °C: Pyrolyze polymer with splitting hydrogen sulfide;
- 4) 340 °C: Release aliphatic compounds and methane and other hydrocarbons;
- 5) 380 °C: Occur carbonization;
- 6) 400 °C: Decompose carbon, oxygen and nitrogen compounds;
- 7) 400 °C to 420 °C: Pyrolyze asphalt for oil and tar production;
- 8) < 600 °C: Crack asphalt materials to produce heat resistance substances;
- 9) > 600 °C : Produce olefins and aromatic compounds;

The pyrolysis process can be categorized as 3 types according to the heating rate applied for decomposition of solid organic substances (Martinez et al., 2013):

- **Slow pyrolysis** is the conventional pyrolysis process which is slow and irreversible to thermally decompose the solid organic substances in the presence of low heating rate (approximately 5-7 °C/min), low temperature and long residence time. The secondary conversion of primary products occurred from the long residence time

induces the high yield of coke. Thus, this process has traditionally been used for the production of charcoal.

- **Fast pyrolysis** is a promising low-cost technology to produce fuels for transportation. It is performed under high heating rates (300-500 °C/min) with rapidly quenching of volatiles to form liquid products (up to 70 wt%). This also benefits to terminate the secondary conversion of the obtained products.

- **Flash pyrolysis** is carried out under high heating rate of 1000°C/min in the absence of oxygen to decompose organic materials with the purpose of creating specific chemical reactions. This process requires short residence time for pyrolysis (few seconds) at moderate temperatures (400-650 °C).

2.6 Pyrolysis of Waste Tire

Pyrolysis of waste tire is the practicable technique to produce alternative liquid fuels which are expected to replace the conventional ones. These liquid fuels typically have high heating values in the range of 40-50 MJ/kg. In addition, pyrolysis permits the recovery of the high grade steel and carbon in the form of smokeless solid fuel, carbon black, or activated charcoal (Hayworth et al., 1995). In the pyrolysis of waste tire, the large hydrocarbon chains are broken down at certain temperatures in the absence of oxygen to give end products usually containing solid char (30-40 wt%), liquid products (40-60 wt%) and gases (5-20 %) (Juma et al., 2006). The liquid products are consisted of a various complex mixture of organic components. Thus, the derived liquid products may be directly used as fuels, petroleum refinery feedstock or a source of chemicals. The gaseous fraction is composed of non-condensable organic substances such as H₂, H₂S, CH₄, C₂H₄, C₃H₆ etc (Juma et al., 2006), which can be applied as gaseous fuel in the pyrolysis process. The details of pyrolysis products from waste tire pyrolysis are given below:

- **Solid residue** contains carbon black, high boiling points tar, inorganic ash and some mineral matters generated from vulcanizing agents. This solid residue are also called as “tire char”. Ariyadejwanich et al. (2003) reported the possibility to use this char obtained from waste tire pyrolysis as an activated carbon. They found that an activated carbon was firstly produced from waste tires through the

conventional process of carbonization at 500 °C in N₂ atmosphere. Then, the obtained chars were activated using steam at 850 °C to generate the fairly mesoporous activated carbon having mesopore volumes and BET surface area up to 1.09 cm³/g and 737 m²/g, respectively. The activated carbon are widely used as adsorbents in the separation process. It is also widely used for treating wastewater in many industries such as food, textile, chemical and pharmaceutical manufactures.

- **Liquid product** is the main product derived from the waste tire pyrolysis. It can be applied as the fuel oil for industrial and commercial purposes. From analyzing with a gas chromatography/mass spectroscopy (GC/MS), this pyrolysis oil contains broad chemical class fractions, which are consisted of aliphatic, aromatic, hetero-atom and polar fractions. Dai et al. (2001) reported that the compositions found in the waste tire pyrolysis oil produced by a circulating fluidized bed were consisted of 26.8 wt% of alkanes, 42.1 wt% of aromatics, 26.6 wt% of non-hydrocarbon and 4.05 wt% of asphalt. Laresgoiti et al. (2004) characterized the liquid products obtained from waste tire pyrolysis in the fixed bed reactor and reported that the aromatic fraction in the waste tire pyrolysis oil increased from 53.4 to 74.8 wt% when the pyrolysis temperature was increased from 300 to 700 °C and the heating value of the obtained pyrolysis oil (42 MJ/kg) was higher than that of the conventional fuel oil (15-31 MJ/kg). William et al. (2013) have reported that the oil yield derived from the pyrolysis of waste tire reached a maximum at 58.2 wt% when the pyrolysis temperature was 475 °C. Above this point, the oil yield tended to be decreased. However, the increase in the pyrolysis temperature increased the gaseous yield from 4.5 wt % at 450 °C to 8.9 wt% at 600 °C.

- **Gaseous product** generated from the waste tire pyrolysis is mainly composed with incondensable gases such as CO₂, CO, H₂, H₂S, CH₄, C₂H₆, C₃H₆, C₃H₈, and C₄H₆, with other hydrocarbon gases in diluted concentration (Juma et al., 2006). The composition of the pyrolysis gas is depended on various factors. Although the pyrolysis process is supposed to be operated in an oxygen free environment, the non-condensable gas still contains oxides of carbon due to the oxygenated compounds in the waste tire itself such as some organic acids (stearic acid) and inorganic oxides (zinc oxide and iron oxides). At low pyrolysis temperature, the organic acids may be cracked to form oxides of carbon and oxygenated organic compounds. At high temperature, the inorganic oxides is dissociated to form carbon oxides and oxygenated organic

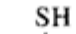

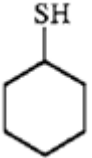
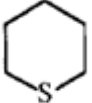

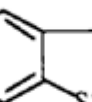

compounds. At severe pyrolysis conditions, high temperature with fast heating rate induces the formation of larger fractions of lighter hydrocarbons and hydrogen gases.

2.7 Sulfur Compounds in Waste Tire Pyrolysis Oil Compared to Petroleum Products (Matar and Hatch, 1994)

Various type of important non-hydrocarbon compounds found in the crude oil and refinery streams involves with the groups of the organic sulfur, nitrogen and oxygen compounds. Trace of metallic compounds are also found in all crudes. The presence of these impurities is harmful and may cause problems for catalytic processes. Fuels having high sulfur and nitrogen levels can cause pollution and their oxidized products also have the corrosive nature. Sulfur in crude oil is mainly presented in the form of organosulfur compounds. Hydrogen sulfide (H_2S) is the only important inorganic sulfur compound containing in the crude oil. The organosulfur compounds are generally classified as acidic and non-acidic substances as shown in Table 2.4. The acidic sulfur compounds involve thiols (mercaptans). Thiophene, sulfides and disulfides are classified in the group of non-acidic sulfur compounds normally found in the crude oil fractions. Moreover, the corrosive sulfur compounds have an obnoxious odor. Pyrophoric iron sulfide is produced from the corrosive action of sulfur compounds on the iron or steel used in refinery process equipment, piping, and tanks. The combustion of petroleum products containing these sulfur compounds releases undesirable products such as sulfuric acid and sulfur dioxide.

The different boiling points of sulfur compounds in the crude oil is resulted from the different composition and type of sulfur compounds. In gasoline, more than 90% of the sulfur compounds are in the form of thiophene and its derivatives, while the sulfurous components in diesel are mainly consisted of thiophenic substances (70-80%) such as alkylbenzothiophenes and alkyldibenzothiophenes. The major compounds were dibenzothiophene derivatives with alkyl groups at 4 and/or 6-position including 4-methyldibenzothiophene (4-MDBT), 4,6-dimethyldibenzothiophene (4,6-DMDBT), 3,6-dimethyl dibenzothiophene (3,6-DMDBT) and 2,4,6-trimethyldibenzothiophene (2,4,6-TMDBT) (Ma et al., 2002).

Table 2.4 Example of Some Sulfur Compounds in Crude Oil (Matar and Hatch, 2012)

Type of sulfur compounds	Sulfur compounds	Structure
Acidic sulfur compounds	Methyl mercaptan	CH_3SH 
	Phenyl mercaptan	
	Cyclohexylthiol	
Non-acidic sulfur compounds	Dimethylsulfide, Dimethyldisulfide	CH_3SCH_3 , $\text{CH}_3\text{S-CH}_3$ 
	Thiocyclohexane	
	Thiophene	
	Benzothiophene	

Each crude oil has different amounts and types of sulfur compounds depended on geological environment of source, depth of the individual well, time and substrates to form crude oil as shown in Table 2.5. Generally, the higher density of crude oil with the lower API gravity has the higher sulfur content.

Table 2.5 Characteristics of Some Typical Crude Oils (Dickey, 1981)

Name of crude oil	Country	Specific gravity ($^{\circ}$ API)	Sulfur content (wt%)	Viscosity (SUS at 38 $^{\circ}$ C)
Smackover	USA	20.5	2.30	270
Kern River	USA	10.7	1.23	6000+
London	USA	38.8	0.26	45
Bradford	USA	42.4	0.09	40
East TX	USA	38.4	0.33	40
Leduc	Canada	40.4	0.29	37.8
Poza Rica	Mexico	30.7	1.67	67.9
Kirkuk	Iraq	36.6	1.93	42
Abqaiq	Saudi Arabia	36.5	1.36	
Boscan	Venezuela	9.5	5.25	

For the waste tire pyrolysis oil, Benallal et al. (1995) found that the light naphtha fraction (distilled at 160 $^{\circ}$ C) in the vacuum oil derived from waste tire pyrolysis at 13 kPa and 500 $^{\circ}$ C had high concentration of sulfurous compounds, identified by using GCMS such as 2-methylthiophene, 3-methylthiophene, 2-ethylthiophene, 2,5-dimethylthiophene, 2,4-dimethylthiophene, 2,3-dimethylthiophene, 3-ethylthiophene, 2-isopropylthiophene, 2-tert-butylthiophene and benzothiazole. Williams and Bottrill (1995) investigated the sulfur-polycyclic aromatic hydrocarbons (PASH) from pyrolytic oil produced from a bench-scale static batch reactor and a fluidized bed reactor at three heating rates to a final pyrolysis temperature of 700 $^{\circ}$ C. The GC-FPD chromatograms of waste tire pyrolysis oil (Figure 2.4) indicated that the major sulfur compounds in the waste tire pyrolysis oil were benzothiophene, dibenzothiophene and its derivatives.

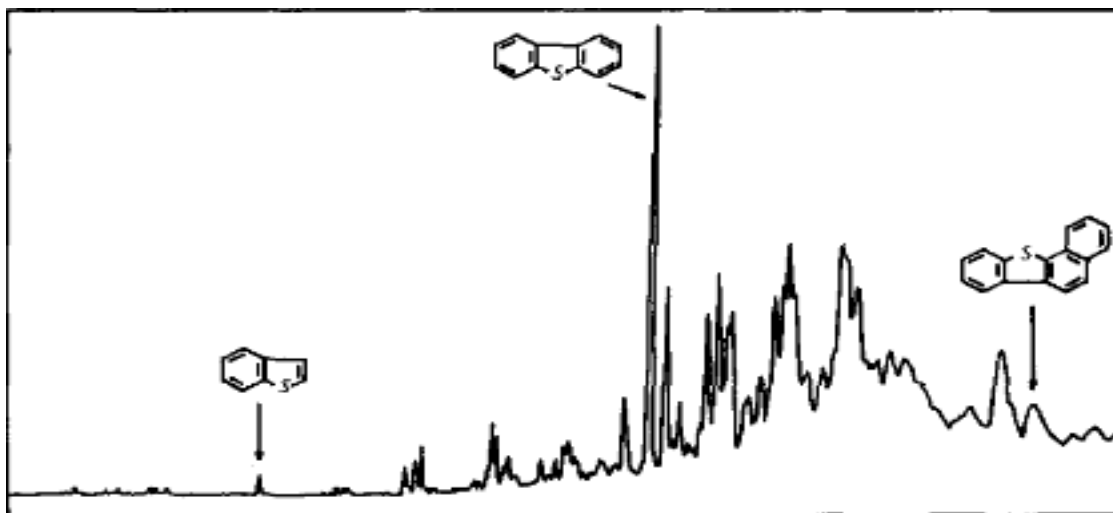


Figure 2.4 GC-FPD Chromatogram of Waste Tire Pyrolysis Oil (Williams and Bott-rill,1995).

2.8 Current Desulfurization Technologies

2.8.1 Hydrodesulfurization (Kowsari, 2013)

Hydrodesulfurization is a kind of a hydrotreating processes, which is one of the most common desulfurization methods applied in refinery processes since the 1950s. Hydrodesulfurization is a catalytic chemical process widely used to remove sulfur (S) from natural gas and from refined petroleum products such as gasoline or petrol, jet fuel, kerosene, diesel fuel, and fuel oils. The purpose of sulfur removal is to reduce the sulfur dioxide (SO₂) emissions from the combustion of these fuels in automotive vehicles, aircraft, ships, gas or oil burning power plants, residential and industrial furnaces. The hydrodesulfurization is normally carried out at high temperature in the range of 300 to 400 °C and high hydrogen pressures from 30 to 130 atm to convert organosulfur compounds as hydrogen sulfide (H₂S) and hydrocarbons. For the industrial section, the hydrodesulfurization processes include facilities for the capture and removal of the resulting H₂S gas. In petroleum refineries, the H₂S gas is then subsequently converted as a by-product elemental sulfur or sulfuric acid (H₂SO₄). The commercial catalysts used for hydrodesulfurization are in sulfide form based on molybdenum (Mo) or tungstain (W) promoted by nickel (Ni) or cobalt (Co) supported on high surface area carriers such as γ -alumina (γ -Al₂O₃). The main active

species of the catalysts used for hydrodesulfurization are based on molybdenum disulfide (MoS_2). At the edges of the MoS_2 crystallites, the Mo center can stabilize a coordinatively unsaturated site (CUS) or an anion vacancy. The sulfur compounds such as thiophene can react to this site and undergo a series of reactions involving both C-S scission and C=C hydrogenation. Thus, the hydrogen provides multiple roles-generation of anion vacancy to remove sulfide, hydrogenation, and hydrogenolysis. A diagram for the cycle is shown in Figure 2.5. The efficiency of hydrodesulfurization is depended on several parameters such as sulfiding protocol, reaction temperature, reaction time, partial pressure of hydrogen, properties of catalyst support, type of promoter and concentration of the sulfur compounds in the fed stream.

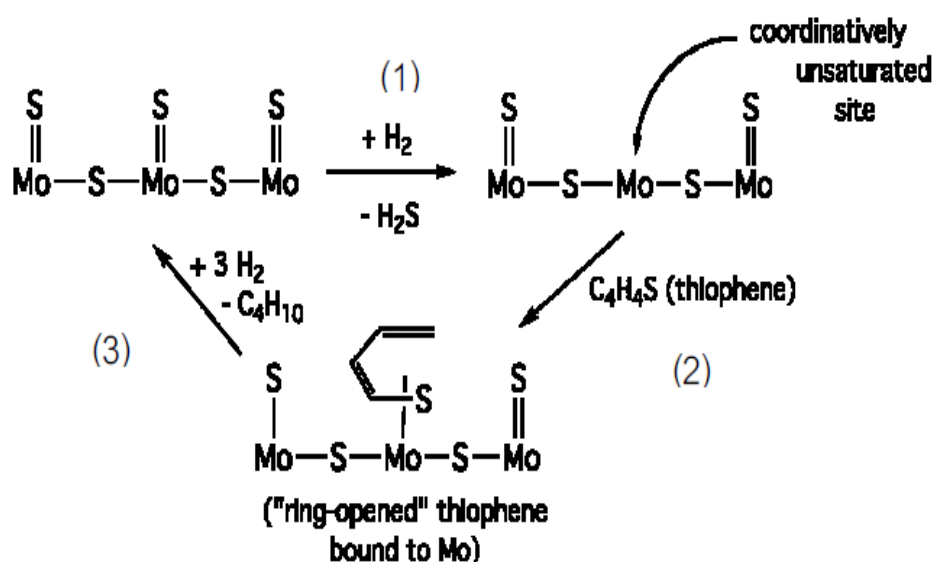


Figure 2.5 Diagram of a Hydrodesulfurization Cycle of Thiophene (Moqadam and Mahmoudi, 2013).

2.8.2 Oxidative Desulfurization (Zhao, 2009)

According to the greater limitation of the sulfur content in the petroleum products, the current requirement to reduce sulfur level in the transportation fuels has shifted the attention of crude oil refiners from the conventional hydrodesulfurization (HDS) to seek other processes. One of such alternative method to achieve this requirement is the oxidative desulfurization in the presence of organic or inorganic peroxides as oxidants. This process offers several advantages over conventional hydroprocess in terms of mild operating conditions and no requirement of valuable hydrogen gas resulting the lower cost of operation. Moreover, the oxidative desulfurization can easily oxidize and remove thiophenic sulfur compounds such as 4,6-dimethyldibenzothiophene (4,6-DMDBT), which is difficult to be removed via hydrodesulfurization due to its stereo hindrance effect around the sulfur atom in the molecule. However, the oxidative desulfurization process requires large amounts of oxidizing agent, separation and recovery of the catalysts including low selectivity and activity towards the sulfur compounds. It is known that this process converts the organosulfur compounds in the fuel as sulfones (or sulfoxides). These polar organic oxides can be removed from the fuels using solvent extraction and/or adsorption. Figure 2.6 shows the simplified oxidative desulfurization scheme for dibenzothiophene (DBT) conversion as dibenzothiophene sulfone through the intermediate dibenzothiophene sulfoxide.

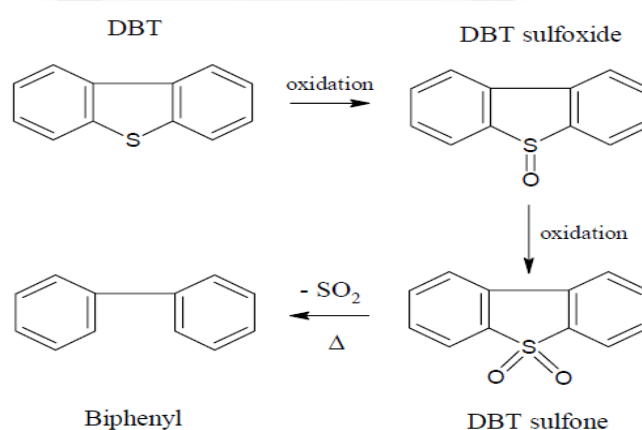


Figure 2.6 Simplified Network for Oxidative Desulfurization of Dibenzothiophene (Zhao, 2009).

2.8.3 Biodesulfurization (Zhao, 2009)

Another method for the removal of sulfur is biocatalytic desulfurization, or biodesulfurization (BDS). Microorganisms require sulfur for growth and several bacteria can utilize the sulfur in thiophenic compounds and thus reduce the sulfur content in petroleum. Biodesulfurization is generally operated under ambient conditions. It mainly proceeds through two biological pathways involving partial or complete degradation of the molecules via C-C bond cleavage or a specific C-S bonds cleavage. The more selective sulfur-specific pathway is preferable to retain the value of fuels. Figure 2.7 illustrates the simplified sulfur-specific enzymatic pathway for the biodesulfurization of dibenzothiophene in the presence of oxygen and water to yield 2-hydroxybiphenyl as non-degradable end-product. Although many bacteria can utilize sulfur through the sulfur-specific pathway, stability and life-time of the biocatalysts have to be concerned. In addition, the cooling system is required to maintain the ambient temperature of the petroleum feedstock and the separation process to remove the biocatalyst. These process can increase the operating cost. Implementation of the biodesulfurization as an industrial process would require microorganisms with higher sulfur removal activity, hydrocarbon phase tolerance, removal ability at high temperatures and longer stability.

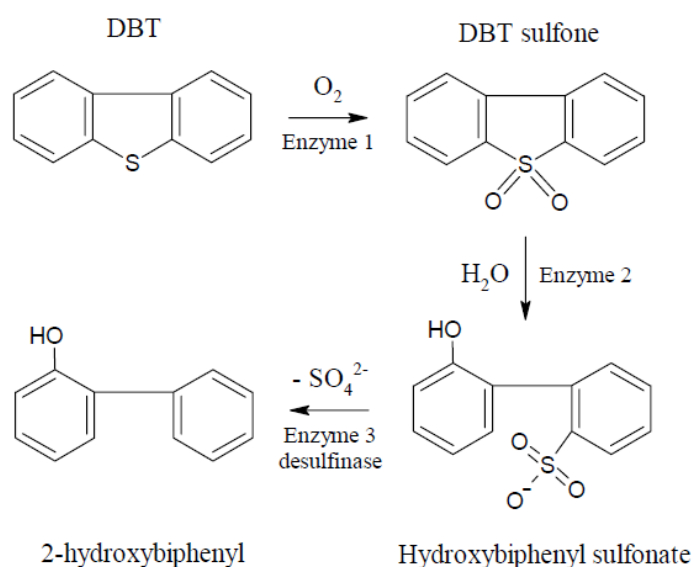


Figure 2.7 Simplified Sulfur-Specific Biodesulfurization of Dibenzothiophene (Zhao, 2009).

2.8.4 Adsorptive Desulfurization

Adsorption is one of the most promising processes for deep desulfurization of fuels. This process is effective in the selective removal of low-concentration materials from liquids. The fuel is brought to contact with a solid adsorbent, which selectively adsorbs sulfur containing compounds. This process can generate ultra-low sulfur concentration fuel with insignificantly affecting the fuel properties. Moreover, it does not consume hydrogen and it can be operated at ambient or rather low temperature and pressure. This process is divided into two groups: adsorptive desulfurization and reactive adsorption desulfurization (Khodadadi et al., 2012). Adsorptive desulfurization is based on a physical adsorption of organosulfur compounds on the solid sorbent surface. Regeneration of the used sorbent with a desorbent resulting in a high concentration of sulfur compounds in the exit flow. Whereas, the reactive adsorption desulfurization is a reaction of the organosulfur compounds on the sorbent. The fixed sulfur on the sorbent is usually in the sulfide form. The desulfurization performance is generally depended on the adsorption dynamics and the amount of sorbent. The general adsorbents applied for the adsorption of the sulfur compounds in the liquid hydrocarbons are activated carbons, activated aluminas and zeolites.

2.8.5 Photocatalytic Desulfurization (Anpo and Kamat, 2010)

Photocatalytic desulfurization is a new process to remove the sulfur compounds in fuels. Its advantage is related to the energy saving to reduce operating cost. The organic sulfur compounds are known to undergo the photochemical degradation and oxidation even in the absence of any photosensitizer or photocatalyst. Absorption of a quantum of ultraviolet light by sulfides and disulfides is considered to produce the cleavage of a C-S or S-S bonds. For the photocatalytic desulfurization, the reaction divided into two stages. The first stage involves with the transfer of sulfur-containing compounds contained in the light oil to a polar extraction solvent. Then, the extracted sulfurous compounds were photo-oxidized by photons generated from the light source and catalysts. Photocatalytic reactions are often carried out with mercury lamps as a light source. Low pressure mercury lamps mainly emit at 254 nm, whereas the medium pressure mercury lamps emit at 254, 365 nm and many other bands. Photocatalysis over TiO_2 requires wavelengths shorter than 400 nm. The direct

photolysis of sulfur compounds can proceed under irradiation of 254 nm band of mercury lamps.

2.9 Literature Reviews

Chang (1996) studied the non-catalytic pyrolysis of waste tire and focused on the degradation rate and product yields. All the pyrolysis experiments were performed under isothermal conditions with atmospheric pressure. The pyrolysis temperature varied from 200-800 °C. The conversion level of waste tire at 400 °C reached to 95% in 2 min. The result indicated that the pyrolysis of waste tire was a fast degradation due to its high content of volatiles matter (62.3%). The degradation rate of waste tire increased with increasing the pyrolysis temperature as a result of thermodynamics. Pyrolysis or thermal cracking was classified as an endothermic reaction requiring high energy to crack the chemical bonds of polymers in tire. Therefore, the high pyrolysis temperature promoted the progress of the reaction. However, the pyrolysis conversion was not greatly increased by increasing the pyrolysis temperature above 400°C. The product yields of gas, oil and char were in the range of 30-53 wt%, 28-42 wt% and 14-28 wt%, respectively. At 350 °C, the fuel oil, which was a part of the oil production, had the maximum level up to 15 wt%.

Kwak et al. (1999) investigated the hydrodesulfurization activity of dibenzothiophene (DBT) and 4,6-dimethyldibenzothiophene (4,6-DMDBT) by using phosphorus-added CoMoS₂/Al₂O₃ catalysts. Hydrodesulfurization of both reactants was carried out in a 100 cm³ autoclave at 623 K under 40 MPa of hydrogen pressure. The effect of phosphorus addition exhibited the enhancement of the Mo species dispersion and Brønsted acidity. The increase in the Brønsted acidity reduced the effect of steric hindrance of 4,6-DMDBT due to the migration of the methyl groups. The maximum conversion (75%) of hydrodesulfurization was obtained when the proper phosphorus content in the catalyst was loaded as 0.5 wt%.

Boxiong et al. (2007) investigated the pyrolysis of waste tire by using zeolite ultrastable Y-type (USY) as a catalyst. The pyrolysis of waste tire was carried out in a two-stage bed reactor. The waste tire was firstly pyrolyzed in a fix bed reactor, and then the pyrolysis gases were passed through a secondary catalytic reactor filled with zeolite USY catalyst. The light fraction (boiling point < 220 °C) from pyrolysis was

analyzed by gas chromatography/mass spectrometry (GC/MS). The result indicated that the presence of zeolite USY catalyst reduced the oil yield with increasing the gas products. This catalyst also promoted the formation of certain single ring of aromatic compounds such as benzene, toluene and the *m*-, *p*-, and *o*-xylenes. When catalyst/tire ratio was increased, the whole yield of oil decreased with the reduction of the total amount of aromatic hydrocarbons. The amount of benzene, toluene or xylenes reached the maximum value at 8.15, 26.3 and 21.5 wt% respectively, when the catalyst/tire ratio was 0.5.

Yu et al. (2008) investigated the hydrodesulfurization of thiophene by using Co, Mo, NiMo and CoMo supported on alumina, fishbone and platelet carbon nanofibers (CNFs) as catalysts. The results indicated that the alumina-supported catalysts gave the higher activity than the corresponding CNFs supported catalysts due to its dispersion as monolayer of the Mo oxides phases. Moreover, the addition of Ni and Co as promoters induced the better dispersion of the Mo oxides which was confirmed by X-Ray Diffraction (XRD) resulting a significant increase in the catalyst activity. Although the alumina-supported catalysts were more difficult to be reduced due to the strong interaction between alumina support and the metal particles, it still showed the higher activity than the CNFs- supported catalysts. Therefore, the dispersion was higher important factor than reducibility for hydrodesulfurization activity. It was also observed that NiMO catalysts were higher active than the CoMo catalyst resulting from the better dispersion of the Mo species in the supported NiMo catalyst. This led the ease of catalyst reduction.

Rinaldi et al. (2010) studied the influence of the addition of citric acid (HCOOH) into the catalyst on the activity for hydrodesulfurization of thiophene. The $\text{MoO}_3/\text{Al}_2\text{O}_3$ catalyst was prepared by a simultaneous impregnation method and a post-treatment method. The results showed that the addition of citric acid by post-treatment method or by simultaneous method were not much affect on the hydrodesulfurization activity and the edge dispersion of MoS_2 at low Mo content (8.7 wt%). In contrast, at a high Mo content (>20 wt%), the addition of citric acid by post-treatment method improved the edge dispersion of MoS_2 on the catalyst surface and decreased the interaction between Mo and support to increase the sulfidation degree of Mo to consequently promote the hydrodesulfurization activity of thiophene.

Deng et al. (2010) reported the hydrodesulfurization of straight-run diesel in a slurry reactor by using a $\text{NiMoS}_2/\text{Al}_2\text{O}_3$ catalyst. The operating conditions were 4.8-23.1 wt% catalyst under the reaction temperature in the range of 320-360 °C and 3-5 MPa of hydrogen pressure with 0.56-2.77 L/min of hydrogen flow rate. It was found that the hydrodesulfurization activity in the slurry reactor was better than that in a fixed bed reactor.



CHAPTER III

EXPERIMENT AND CHARACTERIZATION

This research work aimed to produce the renewable liquid fuel derived from the waste tire pyrolysis with low sulfur content via hydrodesulfurization catalyzed by using molybdenum supported on γ -alumina ($\text{Mo}/\gamma\text{-Al}_2\text{O}_3$), nickel-molybdenum supported on γ -alumina ($\text{NiMo}/\gamma\text{-Al}_2\text{O}_3$) and cobalt-molybdenum supported on γ -alumina ($\text{CoMo}/\gamma\text{-Al}_2\text{O}_3$). The experiment was divided into five steps:

1. Preparation and characterization of the waste tire powder
2. Pyrolysis of the waste tire powder and characterization of its products
3. Preparation and characterization of catalysts
4. Investigation of the effect of reaction conditions applied in the hydrodesulfurization of the waste tire pyrolysis oil on the level of sulfur removal
5. Characterization of the hydrodesulfurized waste tire pyrolysis oil properties

3.1 Materials

The waste tire powder ($\text{Ø} = 250 \mu\text{m}$) was received from Unioin Commercial Development Co., Ltd. (Samutprakarn, Thailand). The chemicals used for the synthesis of the catalysts were activated $\gamma\text{-Al}_2\text{O}_3$ (surface area = $119.0 \text{ m}^2/\text{g}$) ($\text{Ø} = 150 \mu\text{m}$) (KHD-12, Sumitomo Chemical Co., LTD., Japan), ammonium tetrathiomolybdate ($[\text{NH}_4]_2\text{MoS}_4$, ATTM) (Aldrich, 99.97%), cobalt nitrate hexahydrate ($\text{Co}(\text{NO}_3)_2 \cdot 6\text{H}_2\text{O}$) and nickel nitrate hexahydrate ($\text{Ni}(\text{NO}_3)_2 \cdot 6\text{H}_2\text{O}$) (QRec, 97%). Hydrogen gas (99.99% purity, Praxair) was used for the reduction of catalyst and hydrodesulfurization. Nitrogen gas (99.99% purity, Praxair) was used for pyrolysis of the waste tire powder. Air (99.95% purity, Praxair) and helium (99.95% purity, Praxair) were also used for analysis by gas chromatography equipped with a flame photometric detector (GC-FPD).

3.2 Experimental Procedures

3.2.1 Pyrolysis Process

Figure 3.1. shows a schematic diagram of pyrolysis process. The waste tire powder (100 g/batch) was pyrolyzed in a stainless steel tubular fixed bed reactor placed in the tubular furnace with a heating rate of 25 °C/min. The pyrolysis temperature was given as 400 °C (referring from the thermogravimetric analysis (TGA) results reported in the section of 3.3.1) under a nitrogen atmosphere at a flow rate of 0.1 L/min for 10 min. The obtained vapor from pyrolysis was condensed in the Erlenmeyer flasks immersed in an ice bath. This oil fraction was called as “condensed oil”. When the fixed bed reactor was removed from the tubular furnace, the residual products in the reactor were washed with tetrahydrofuran (THF) to extract heavy fraction from char and called as “residual oil”. The amount of gas fraction was calculated by the percentage difference in weight.

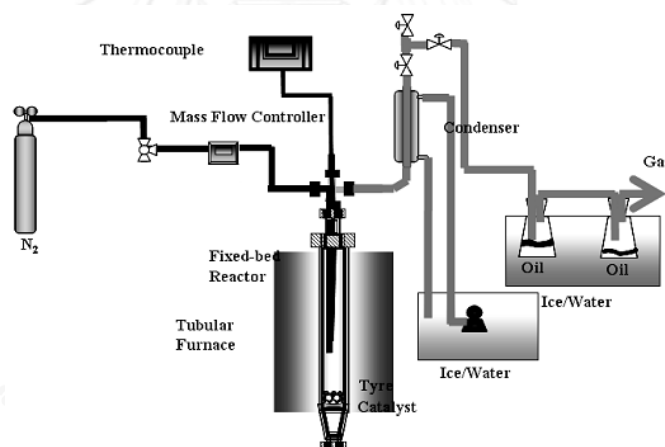


Figure 3.1 Schematic Diagram of Pyrolysis Process.

3.2.2 Catalyst Preparation

All of the catalysts were prepared by the successive incipient wetness impregnation method (Xiang et al., 2008). For preparation of Mo/ γ -Al₂O₃, the γ -Al₂O₃ was dried in an oven at 100 °C for 24 h. [NH₄]₂MoS₄ (ATTM) dissolved in de-ionized (DI) water (0.77M) was then impregnated on the dried γ -Al₂O₃. The obtained product was then dried in an oven at 60 °C for 12 h and calcined at 250 °C for 3 h. The calcined

product was further impregnated with 1.02 M of $\text{Ni}(\text{NO}_3)_2 \cdot 6\text{H}_2\text{O}$ or $\text{Co}(\text{NO}_3)_2 \cdot 6\text{H}_2\text{O}$ solution to produce the $\text{NiMo}/\gamma\text{-Al}_2\text{O}_3$ or $\text{CoMo}/\gamma\text{-Al}_2\text{O}_3$ catalysts. The resulting products were dried at the same condition as described above and then calcined at 500 °C for 3 h.

3.2.3 Hydrodesulfurization of Waste Tire Pyrolysis Oil

The hydrodesulfurization of the waste tire pyrolysis oil was carried out in a high pressure stirring reactor (250 mL). In the reduction step, the reactor containing 0.05 g of catalyst in the presence of decane (10 g) was sealed and purged with hydrogen gas by pressurizing up to 20 bar. Under hydrogen atmosphere, the catalyst in the reactor was reduced at 400 °C for 3 h. After reduction, the temperature was decreased below 100 °C to avoid the evaporation of waste tire pyrolysis oil and then 10 g of waste tire pyrolysis oil was charged into the reactor by syringe. The reactor was agitated under 150 rpm at desired reaction temperature and time. To terminate the reaction, the reactor was immediately quenched in a cold-water bath.

3.3 Analytical Methods

3.3.1 Characterization of Waste Tire Powder and its Pyrolysis Oil

The waste tire powder was controlled to be smaller than 250 microns before characterization. The proximate analysis was evaluated following ASTM D3173-D3175 to detect the levels of moisture, volatile matter, ash and fixed carbon of waste tire powder. The ultimate analysis was evaluated following ASTM D3176-89 to detect the total carbon, hydrogen and nitrogen contents by using CHN analyzer (Perkin Elmer, PE-2400). Total sulfur content of waste tire powder was determined by using the LECO SC-132 Sulfur Determinator (LECO Corporation, St Joseph, Michigan). The oxygen content was then calculated by the percentage of difference. The thermal analysis of waste tire powder was evaluated by using the thermogravimetric/differential thermal analyzer (TG/DTA) (Perkin Elmer, Pyris diamond) to detect the level of decomposition (%weight loss) as a function of increasing temperature. The heating value was also evaluated following ASTM D2015 by using a bomb calorimeter (Parr-6200).

3.3.2 Catalyst Characterization

3.3.2.1 BET Surface Area

The surface area, total pore volume and average pore diameter of the catalysts were detected by using Autosorb-1, Quantachrom. The surface area was calculated from N₂ physisorption using the Brunauer-Emmet-Teller (BET) equation. Average pore size was obtained by the Barrett-Joyner-Halenda (BJH) method in the desorption stage.

3.3.2.2 Scanning Electron Microscopy/Energy Dispersive X-ray Spectroscopy (SEM/EDX)

The surface morphology of catalysts after calcination was investigated by using SEM (JEOL JSM-6400) scanning microscope operated at an accelerating voltage of 15 kV. Before analysis, the catalysts were sputter-coated with gold for increasing a conductivity.

3.3.2.3 X-Ray Diffraction (XRD)

The catalysts after calcination were characterized by XRD diffractometry using a Bruker D8 Advance XRD system employing CuK α radiation ($\lambda = 1.5406 \text{ \AA}$) and an X-ray power of 40 kV, 40 mA. The measurement started from $2\theta = 10^\circ$ to 100° with scanning step of 0.0197 and a count time of 1 second to identify the type and dispersion of crystalline on the surface of the catalysts. Peaks were identified by comparison with standard in a database.

3.3.2.4 Temperature Programmed Reduction (TPR)

The reduction temperature of catalysts was evaluated by temperature programmed reduction (TPR) using gas chromatography (Shimadzu-2014). The TPR instrument consisted of a flow-control system, a thermal conductivity detector (TCD) and a programmed heating unit. A thermal conductivity detector (TCD) was used to measure changes of the thermal conductivity of the gas stream. The TCD signal was then converted to concentration of active gas using a level calibration. The integrated area under the profile of concentration vs. temperature yields the total consumed gas volume. TPR was under hydrogen/nitrogen (5% (v/v)). 0.1 g of each

calcined catalyst was placed in a reactor. At the pre-treatment step, TPR was under nitrogen atmosphere at a flow rate of 30 mL/min and 100 °C for 30 min to remove impurities and water. The reduction step in the presence of hydrogen gas at a flow rate of 30 mL/min was then operated from ambient temperature to 900 °C with a heating rate of 10 °C/min.

3.3.2.5 Temperature Programmed Desorption (TPD)

The acidity of the catalyst was analyzed by using ammonia TPD analysis carried out in TPDRO/MS 1100. Before evaluation, the catalyst samples were treated under flowing hydrogen gas (20 mL/min) at 300 °C for 2 h to remove water and impurities on the catalyst surface. Pulses of ammonia (10% in helium) were then injected into the reactor at room temperature. The amount of ammonia eluted from the reactor was determined by mass spectrometer. The temperature to desorb the ammonia in the catalyst sample was raised to 1000 °C at a heating rate of 10 °C/min. The desorption peak of ammonia was monitored by using a mass spectrometer.

3.3.3 Type and Content of Sulfurous Compounds in the Waste Tire Pyrolysis Oil

The sulfur content and its species in the waste tire pyrolysis oil before and after hydrodesulfurization were analyzed by using gas chromatography flame photometric detector (GC-FPD) (Shimadzu GC-14B). BP 5 capillary column (30 m x 0.32 mm inner diameter (ID), 0.25 µm film thickness) was used for sulfurous compounds separation. The oil samples were diluted in decane to 5 wt% and then injected into the GC-FPD at 250 °C. The GC oven temperature was programmed to rise from 35 °C (held for 10 min) to 130 °C at a heating rate of 15 °C/min and thereafter to 220 °C at a heating rate of 10 °C/min. The carrier gas was helium with a flow rate of 50 mL/min. The detector operated at 250 °C with an air/hydrogen flame, for which the air and hydrogen gas pressures were 0.74 and 0.98 bar, respectively.

The influence of various parameters on the degree of hydrodesulfurization of the pyrolysis oil derived from waste tire can be calculated following eq. 3.1:

$$\% \text{Sulfur removal} = \left[\frac{C_0 - C_1}{C_0} \right] \times 100 \quad (3.1)$$

where:

- C_0 = Total area of sulfur content in the waste tire pyrolysis oil before hydrodesulfurization analyzed by GC-FPD
- C_1 = Total area of sulfur content in the waste tire pyrolysis oil after hydrodesulfurization analyzed by GC-FPD

3.3.4 Quality of Waste Tire Pyrolysis Oil after Hydrodesulfurization

3.3.4.1 Gas Chromatography Simulated Distillation (GC-SIMDIS)

The waste tire pyrolysis oil before and after hydrodesulfurization, diesel and gasoline were analyzed by using a GC-SIMDIS (Agilent, 6890N) equipped with a flame ionization detector and using simdis HT capillary column (5 m x 530 μ m inner diameter (ID), 2.65 μ m film thickness) to separate individual hydrocarbon components in the order of their boiling points range. The GC-SIMDIS analysis followed ASTM D 2887-2893 to provide a quantitative percent mass yield as a function of boiling point of the hydrocarbon components of samples. The sample was diluted in carbon disulfide (1:1 by volume). 0.1 μ L of sample was injected at 298 $^{\circ}$ C and oven temperature was programmed to rise from 35 $^{\circ}$ C to 350 $^{\circ}$ C at a heating rate of 15 $^{\circ}$ C/min. The detector operated at 320 $^{\circ}$ C and the carrier gas was helium (1.5 mL/min).

3.3.4.2 Gas Chromatography/Mass Spectroscopy (GC/MS)

The waste tire pyrolysis oil before and after hydrodesulfurization were diluted in hexane (0.01 wt%) and performed on a gas chromatography mass spectrometer (Shimadzu-2010) using DB-5 column for separation and indication of the types of multiple compounds in the waste tire pyrolysis oil. The sample (1 μ L) was injected at 230 $^{\circ}$ C and oven temperature was programmed to rise from 40 $^{\circ}$ C (hold 2 min) to 180 $^{\circ}$ C (hold 8 min) at a heating rate of 15 $^{\circ}$ C/min. The detector operated at 250 $^{\circ}$ C and the carrier gas was helium (1.52 mL/min).

3.3.4.3 Viscosity, Copper Strip Corrosion, Heating Value and Iodide Value

The analysis of copper strip corrosion property and viscosity of the waste tire pyrolysis oil followed ASTM D 130 and ASTM D 445 respectively. The heating value of the hydrodesulfurized waste tire pyrolysis oil was also investigated following ASTM D2015. The analysis of iodine value was used to determine the amount of unsaturation (double bonds) in the waste tire pyrolysis oil by using the compact tritator (G20). 0.1 g of waste tire pyrolysis oil was mixed with Wij 'solution (10 mL) and the mixture of cyclohexane and acetic acid (40 mL) and spin for 5 min. The obtained solution was then added with potassium iodide (10 mL) to titrate the double bonds in the waste tire pyrolysis oil.

CHAPTER IV

RESULT AND DISCUSSION

4.1 Characterization of Waste Tire Powder

Table 4.1 showed the composition of waste tire powder from proximate and ultimate analyses. For the proximate analysis, it indicated that the waste tire powder had a large content of volatile matter (57.5 wt%) possibly due to the decomposition of natural and synthetic rubbers in the waste tire. Moreover, the waste tire powder had low moisture content (0.80 wt%) with 17.0 wt% ash and 24.7 wt% fixed carbon. From the ultimate analysis, the waste tire powder had a large amount of carbon (70.0 wt%) with high hydrogen content (6.79 wt%) resulting higher heating value (32.3 MJ/kg) than the biomass such as rice husk (13-16 MJ/kg) (Natarajan et al., 1998) or palm (18-20 MJ/kg) (Vijaya et al., 2004). However, the waste tire powder also contained 1.53 wt% of sulfur obtained from vulcanization of tire production.

Table 4.1 Composition of Waste Tire Powder Feedstock

Analysis	Values
<u>Proximate analysis (wt%)</u>	
● Volatiles	57.5
● Fixed carbon	24.7
● Ash	17.0
● Moisture	0.80
<u>Ultimate analysis (wt%)</u>	
● Carbon	70.0
● Hydrogen	6.79
● Nitrogen	0.28
● Sulfur	1.53
● Oxygen	4.4
Heating value (MJ/kg)	32.3

Moreover, the waste tire powder was also analyzed by the thermogravimetric analysis (TGA) under nitrogen atmosphere at a heating rate of 10 °C/min to determine the weight loss characteristics of waste tire powder. Figure 4.1 showed the TGA thermogram of waste tire powder. The result indicated that the waste tire powder was decomposed by heat about 65 wt% and the remaining (35 wt%), which was not decomposed as the char. Figure 4.1 also showed the waste tire powder had the decomposition temperature in a range from 200 to 500 °C, which an initial decomposition temperature about 250 °C and the maximum decomposition temperature about 370 °C. Thus, the pyrolysis temperature was set at 400 °C to completely decompose the waste tire powder. The DTG thermogram showed that the waste tire powder had three decomposition regions. The first region was at 200-300 °C, and was attributed to the degradation or volatilization of additives. The second region (350-480 °C) was assigned to the degradation of natural rubber (NR) and styrene-butadiene rubber (SBR). The final region (450-500 °C) was attributed to the degradation of butadiene rubber (BR) (Choi et al., 2014).

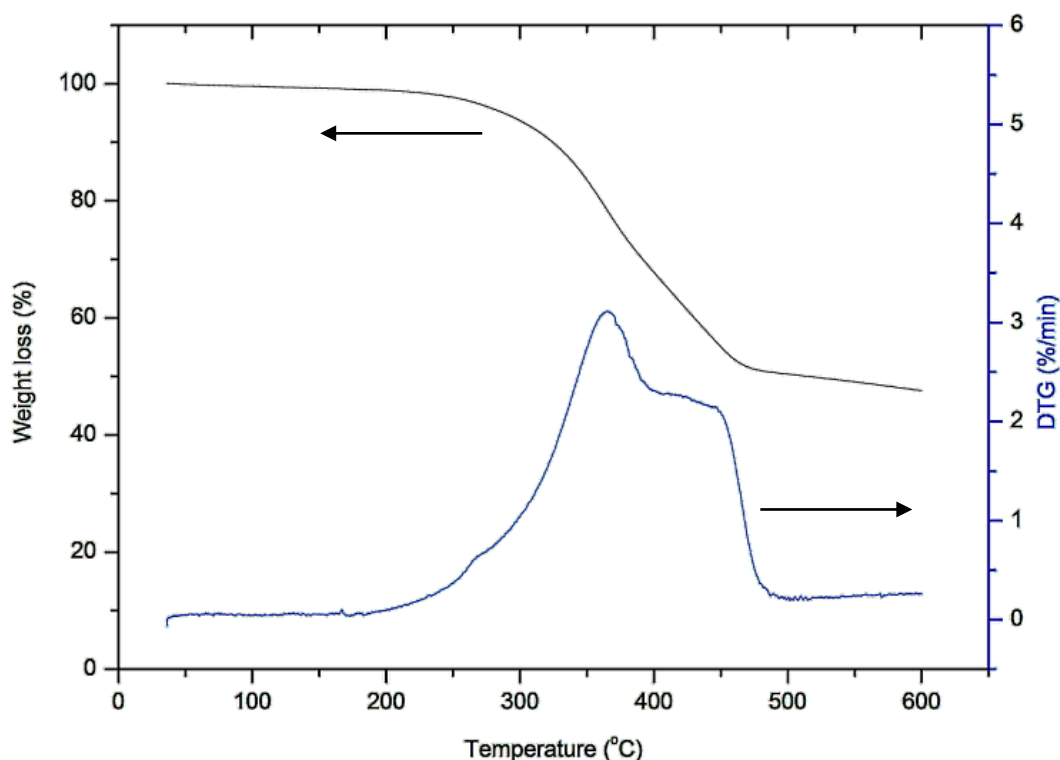


Figure 4.1 TGA Thermogram of Waste tire powder.

4.2 Products Derived from Waste Tire Pyrolysis

The waste tire powder (100 g/batch) was pyrolyzed in a stainless steel tubular fixed bed reactor placed in the tubular furnace with a heating rate of 25 °C/min. The pyrolysis temperature was given as 400 °C under a nitrogen atmosphere at a flow rate of 0.1 L/min for 10 min. The obtained vapor from pyrolysis was condensed in the Erlenmeyer flasks immersed in an ice bath. This oil fraction was called as “condensed oil”. When the fixed bed reactor was removed from the tubular furnace, the residual products in the reactor were washed with tetrahydrofuran (THF) to extract the heavy fraction from char and called it as the “residual oil”. The gas fraction was calculated by the percentage difference in weight. From Table 4.2, this pyrolysis condition gave yields of condensed oil, residual oil, char and gas fractions as 42.0, 4.00, 41.6 and 12.4 wt%, respectively. The condensed oil was the highest fraction, which was more practical to be scaled up than the residual one. Moreover, Table 4.3 shows that the heating value of the condensed oil was 42 MJ/kg, which was higher than that of the waste tire powder (32.3 MJ/kg) due to its higher carbon content. Since the heating value of the waste tire pyrolysis oil was similar to that of diesel fuel (45 MJ/kg) (öner and Altun, 2009), the waste tire pyrolysis oil had potential to replace the conventional crude oil feedstock. However, Table 4.3 shows that the condensed oil fraction had high sulfur content as 1.15% wt% or 31.7 wt% based on the amount of sulfur in the waste tire powder. These sulfur compounds generated from the vulcanizing agents in the waste tire during pyrolysis limits the condensed oil to be directly applied for any combustion engines. Thus, it was necessary to remove the sulfur compounds in the condensed oil obtained from waste tire pyrolysis oil before using or blending with the commercial fossil liquid fuels via hydrodesulfurization.

Table 4.2 Yields of Waste Tire Pyrolysis Products at 400 °C

Pyrolysis Product	Yield (wt%)
Condensed oil	42.0 ± 2.15
Residual oil	4.00 ± 0.50
Char	41.6 ± 0.81
Gas	12.4 ± 1.67

Table 4.3 Ultimate Analysis of Condensed Oil Fraction and Heating Value

Element (wt%)					Heating value (MJ/kg)
Carbon	Hydrogen	Nitrogen	Oxygen	Sulfur	
80.5	7.90	0.52	9.93	1.15	42.0

4.3 Catalysts Characterization

Figure 4.2 showed the schematic diagram of catalyst preparation. All of the catalysts were prepared by the successive incipient wetness impregnation method. For the preparation of Mo/ γ -Al₂O₃ catalyst, the γ -Al₂O₃ support was dried in an oven at 100 °C for 24 h to remove the moisture and impurities. [NH₄]₂MoS₄ (ATTM) dissolved in de-ionized (DI) water (0.77 M) was then impregnated on the dried γ -Al₂O₃ support. The obtained product was then dried in an oven at 60 °C for 12 h and calcined at 250 °C for 3 h (Xiang et al., 2008). The Mo/ γ -Al₂O₃ catalyst was consisted of γ -Al₂O₃ support as a core covered by shell containing the mixture of MoS₄ and MoO₃ with partially releasing of SO₂ during calcination step. To prepare the NiMo or CoMo supported on γ -Al₂O₃, the obtained Mo/ γ -Al₂O₃ powder was then successively impregnated with 1.02 M of Ni(NO₃)₂·6H₂O or Co(NO₃)₂·6H₂O solution, respectively. The resulting products were dried at the same condition as described above and then calcined again at 500 °C for 3 h (Xiang et al., 2008) to obtain the NiO or CoO as the promoter at the outer layer of the obtained catalysts.

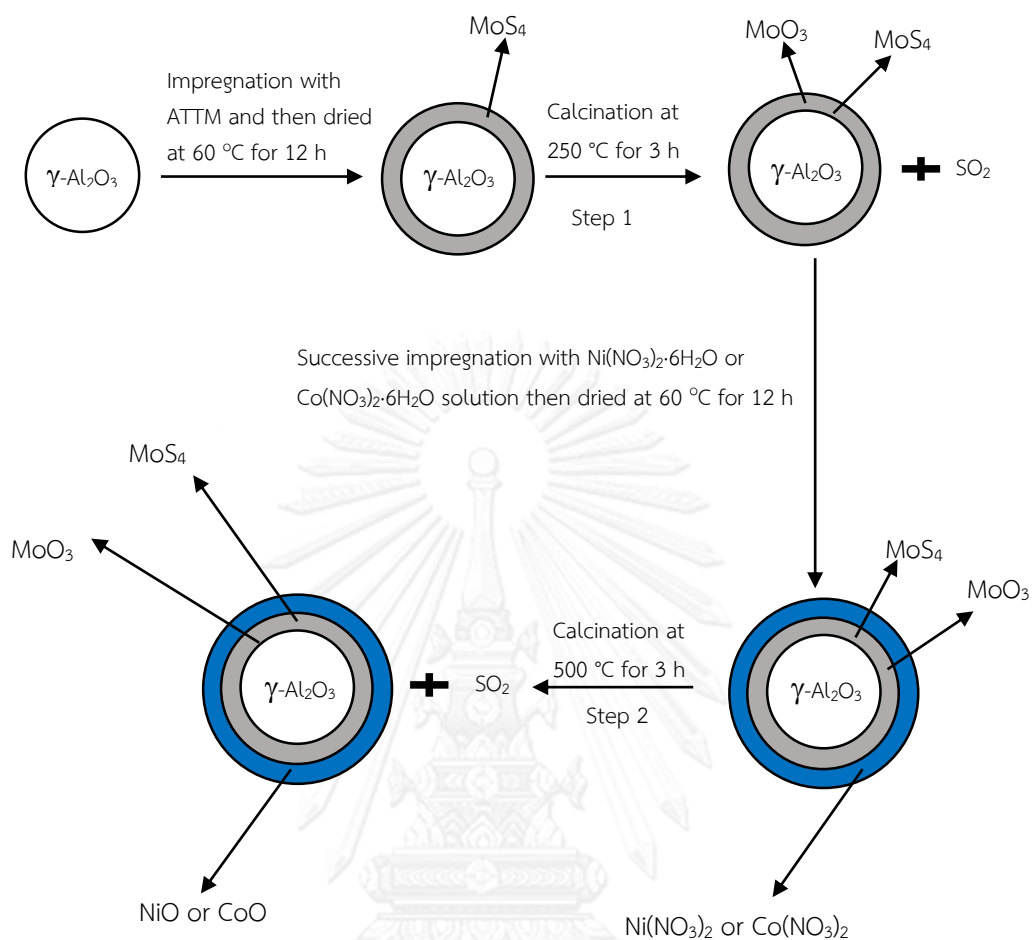


Figure 4.2 Schematic Diagram of Catalyst Preparation.

4.3.1 Scanning Electron Microscopy/Energy Dispersive X-ray Spectroscopy (SEM/EDX)

The SEM/EDX was performed to study the metal dispersion behavior and to evaluate the amount of elemental composition of the prepared catalysts. The instrument was operated in the dark field mode and an overview of the studied catalysts is shown in Figure 4.3a - 4.3e, where the scanned area was marked by the white spots. The amount of elements of each catalyst was also summarized in Table 4.4.

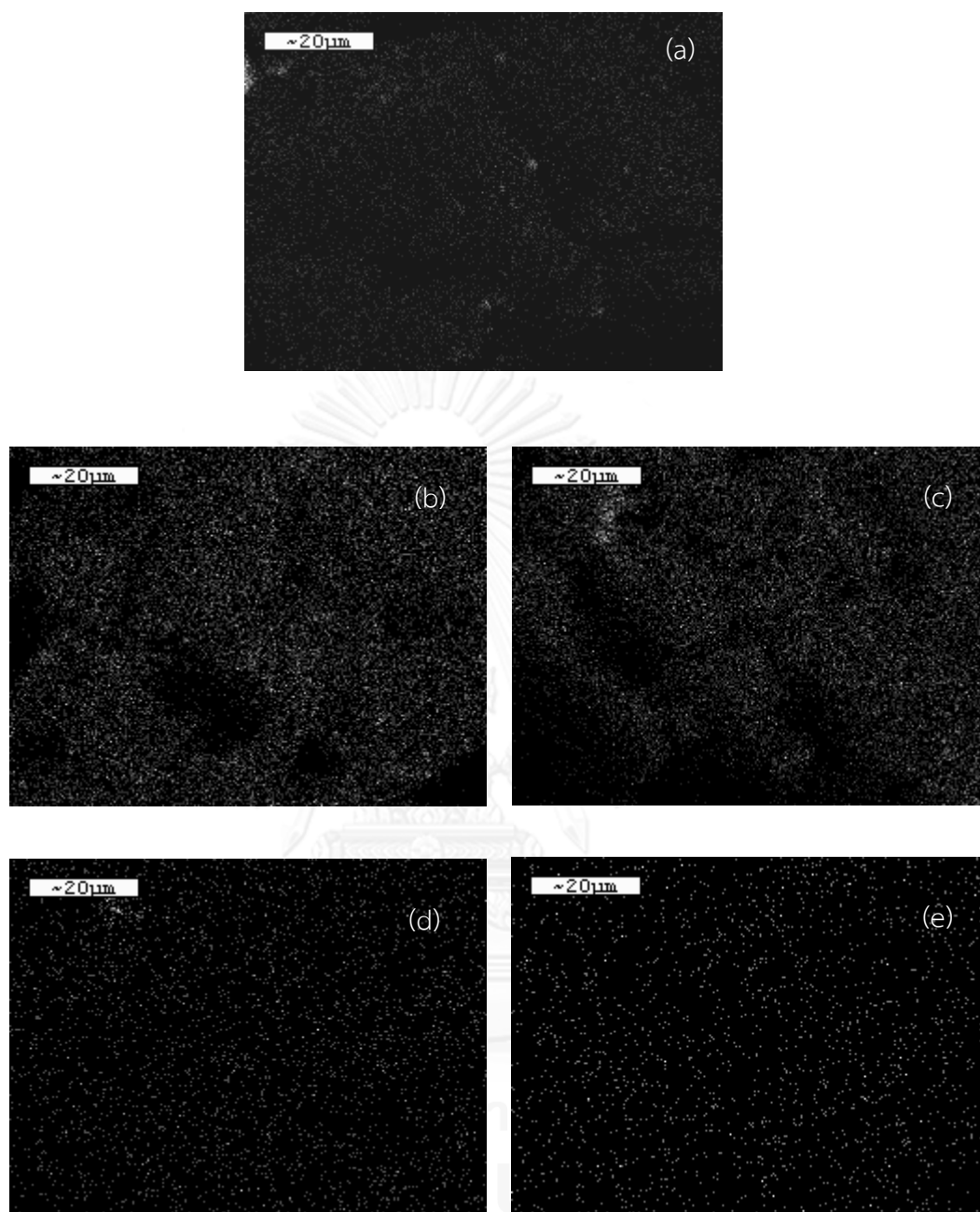


Figure 4.3 SEM/EDX Characterization: (a) Mo Mapping of Mo/ γ -Al₂O₃ Catalyst, (b) Mo Mapping of NiMo/ γ -Al₂O₃ Catalyst, (c) Mo Mapping of CoMo/ γ -Al₂O₃ Catalyst, (d) Ni Mapping of NiMo/ γ -Al₂O₃ Catalyst and (e) Co Mapping of CoMo/ γ -Al₂O₃ Catalyst.

Table 4.4 Elemental Analysis of Each Studied Catalysts

Elements	Mo/ γ -Al ₂ O ₃ (wt%)	NiMo/ γ -Al ₂ O ₃ (wt%)	CoMo/ γ -Al ₂ O ₃ (wt%)
Al ₂ O ₃	93.4	88.2	88.1
Mo	4.34	9.00	8.45
Ni	-	1.69	-
Co	-	-	2.30
S	2.25	1.16	1.15

Without the addition of promoter, Figure 4.3a shows the non-uniform Mo dispersion on the surface of γ -Al₂O₃ support. It was observed that some portion of Mo was agglomerated. Table 4.4 also showed that Mo/ γ -Al₂O₃ catalyst contained only 4.34 wt% Mo content due to incomplete dissolution of ATTM in DI water. When Ni and Co solution was added as the promoter for Mo/ γ -Al₂O₃ catalyst, the higher uniform Mo dispersion with smaller particle size on the γ -Al₂O₃ surface was exhibited as shown in Figure 4.3b or 4.3c, respectively. This result was similar to the previous literatures reported by Gutiérrez et al. (2007) and Tavasoli et al. (2013). Moreover, the addition of Ni or Co also enhanced the amount of Mo on the surface of γ -Al₂O₃ support. This might be explained in that the Ni or Co were interacted with Mo to form NiMoO₄ or CoMoO₄ on the surface of γ -Al₂O₃ support (Lamonier et al., 2005). The comparison of the dispersion of Ni and Co on the surface of γ -Al₂O₃ support was shown in Figure 4.3d and 4.3e, respectively. It was also observed that the dispersion of Ni was more homogeneous with smaller particle size than that of Co on the surface of γ -Al₂O₃ support. This was possible that the higher Co content on the γ -Al₂O₃ surface was easier to be growth as larger particle size inducing the lower dispersion on the γ -Al₂O₃ surface during catalyst preparation. Moreover, the CoMo/ γ -Al₂O₃ catalyst also had atomic ratio of Co/Mo as 0.306 which higher than that of Ni/Mo (0.234) in the NiMo/ γ -Al₂O₃ catalyst. Besides, the amount of S in the NiMo/ γ -Al₂O₃ and CoMo/ γ -Al₂O₃ catalysts was lower than that of Mo/ γ -Al₂O₃ catalyst since some portion of sulfur compounds were lost as SO₂ from calcination steps as shown in Figure 4.2.

4.3.2 BET Surface Area

The adsorption-desorption isotherm of all catalysts were shown in Figure 4.4. The Brunauer-Deming-Deming-Teller (BDDT) classified the gas adsorption isotherms into 5 types (Gregg and Sing, 1967). From the observation in Figure 4.4, the results indicated that the adsorption-desorption isotherm of all catalysts corresponded to type IV isotherm which desorption curves was the characteristics of mesoporous materials (Trakarnpruk et al., 2008). The type IV isotherm revealed both the adsorption volume and the adsorption rate increased with increasing the relative pressure. When the relative pressure exceeded a certain value, the adsorption isotherm was liable to level off. This was closely correlated to the large pore radius in the catalysts (Wang et al., 2012). Furthermore, the type IV isotherm also showed that the adsorption and desorption branches were not coincide, leading the formation of the hysteresis loops. The shapes of the hysteresis loops provided the information of pore structures. From Figure 4.4, the shape of the hysteresis loop of all catalysts showed that they had wide range of pore size distribution (Wang et al., 2012).

Table 4.5 presented the physical properties of all catalysts: Mo/ γ -Al₂O₃, NiMo/ γ -Al₂O₃ and CoMo/ γ -Al₂O₃ prepared via successive wetness impregnation in terms of BET surface area, total pore volume and average pore diameter. The results showed that the Mo/ γ -Al₂O₃ catalyst had the highest values of surface area (96.0 m²/g), largest total pore volume (0.18 cm³/g) and average pore diameter (73.0 Å). After the addition of promoters, a significant reduction of the total pore volume and average pore diameter of NiMo/ γ -Al₂O₃ and CoMo/ γ -Al₂O₃ catalysts were observed. The results indicated that the surface area of NiMo/ γ -Al₂O₃ and CoMo/ γ -Al₂O₃ catalysts decreased to 91.8 m²/g and 81.5 m²/g, respectively.

This result might be due to the enhancement of NiMo and CoMo particle sizes resulted from the condition of impregnation and calcination in the catalyst preparation step (Zepeda et al., 2008). Moreover, the total pore volume and average pore diameter of NiMo/ γ -Al₂O₃ and CoMo/ γ -Al₂O₃ catalysts also decreased in the same trend with surface area due to the deposition of the active species into the pore of catalyst (Zepeda et al., 2008). From the observation, the CoMo/ γ -Al₂O₃ catalyst showed the higher decrease in the surface area, total pore volume and average pore diameter than the NiMo/ γ -Al₂O₃ catalyst resulted from the higher atomic ratio of Co in the CoMo/ γ -Al₂O₃ catalyst.

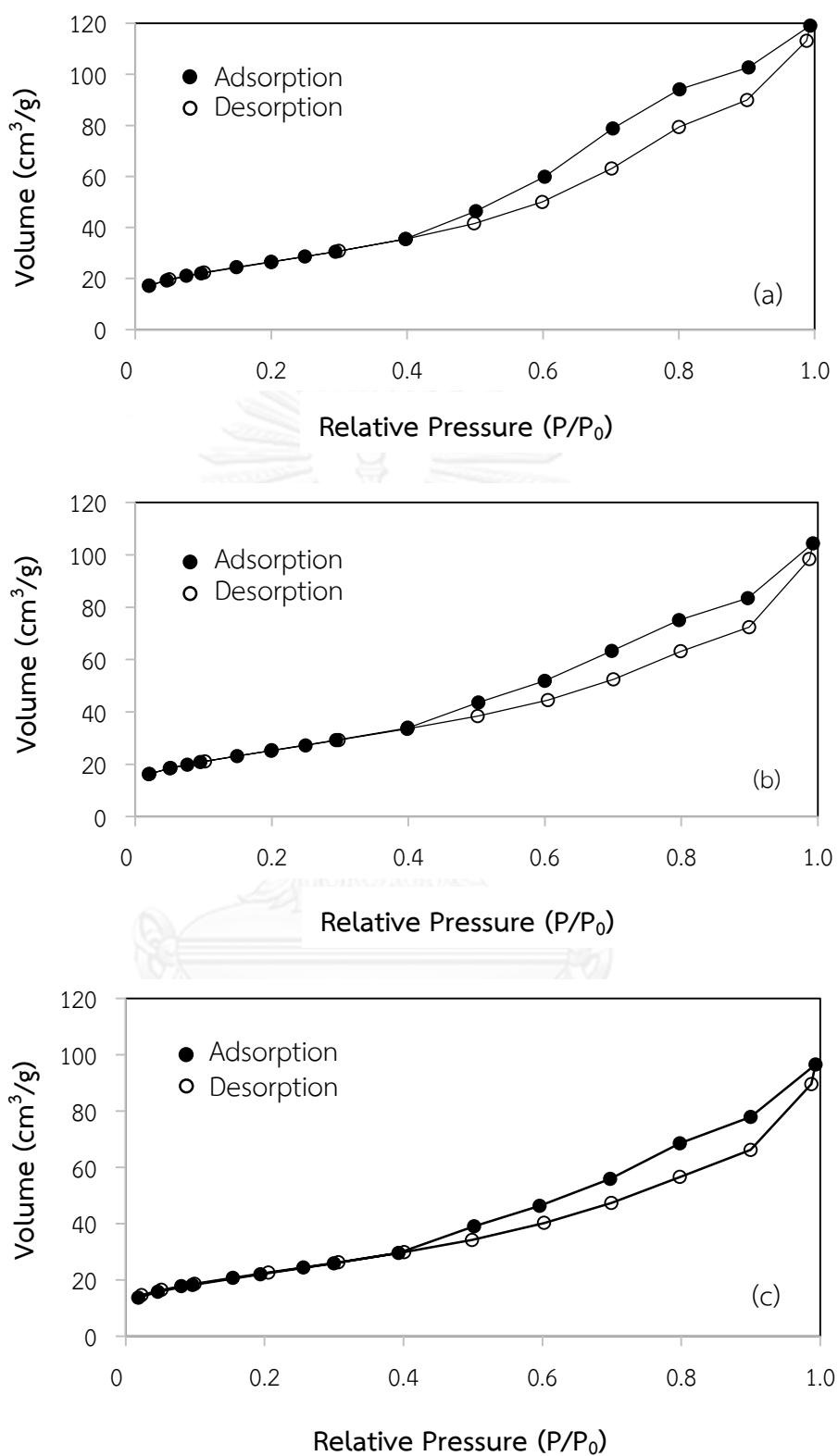


Figure 4.4 Adsorption - Desorption Isotherm of (a) Mo/ γ - Al_2O_3 (b) NiMo/ γ - Al_2O_3 and (c) CoMo/ γ - Al_2O_3 Catalysts.

Table 4.5 BET Surface Area, Total Pore Volume and Average Pore Diameter of Mo/ γ -Al₂O₃, NiMo/ γ -Al₂O₃ and CoMo/ γ -Al₂O₃ catalysts

Sample	Surface area (m ² /g)	Total pore volume (cm ³ /g)	Average pore diameter (Å)
Mo/ γ -Al ₂ O ₃	96.0	0.18	73.0
NiMo/ γ -Al ₂ O ₃	91.8	0.15	68.0
CoMo/ γ -Al ₂ O ₃	81.5	0.13	66.3

4.3.3 X-Ray Diffraction (XRD)

The XRD patterns of Mo/ γ -Al₂O₃, NiMo/ γ -Al₂O₃ and CoMo/ γ -Al₂O₃ catalysts were shown in Figure 4.5. It was found that all catalysts exhibited the diffraction peak of the γ -Al₂O₃ support at 68°. Figure 4.5a presented the XRD pattern of Mo/ γ -Al₂O₃ catalyst. The diffraction peaks of the molybdenum oxide located around at 2 theta of 15°, 28°, 38° and 50° with high intensity. This implied that a large crystalline of molybdenum oxide was formed (Yu et al., 2008). When the promoter (Ni or Co) was loaded onto the Mo/ γ -Al₂O₃ catalyst, the diffraction peaks of separated nickel and cobalt oxides were detected. The XRD patterns of NiMo/ γ -Al₂O₃ and CoMo/ γ -Al₂O₃ catalyst were shown in Figure 4.5b and Figure 4.5c, respectively. The diffraction peaks at 2 theta of 45° (Figure 4.5b) showed the peak for nickel oxide and of 17° and 24° for cobalt oxide (Figure 4.5c). The active structures (Ni–Mo–S or Co–Mo–S phase) were possibly formed as small nano-sized particles, which cannot be detected by XRD method (Yoosuk et al., 2008). The results also showed that the intensity of molybdenum oxide peaks for NiMo/ γ -Al₂O₃ and CoMo/ γ -Al₂O₃ catalysts were significantly decreased after the addition of promoters. It implies that the addition of Ni or Co as the promoters suppressed the growth of molybdenum particle to obtain the small particle size leading the better dispersion of the molybdenum species on the surface of γ -Al₂O₃ support (Tavasoli et al., 2013). This result was also agree with the SEM/EDX analysis.

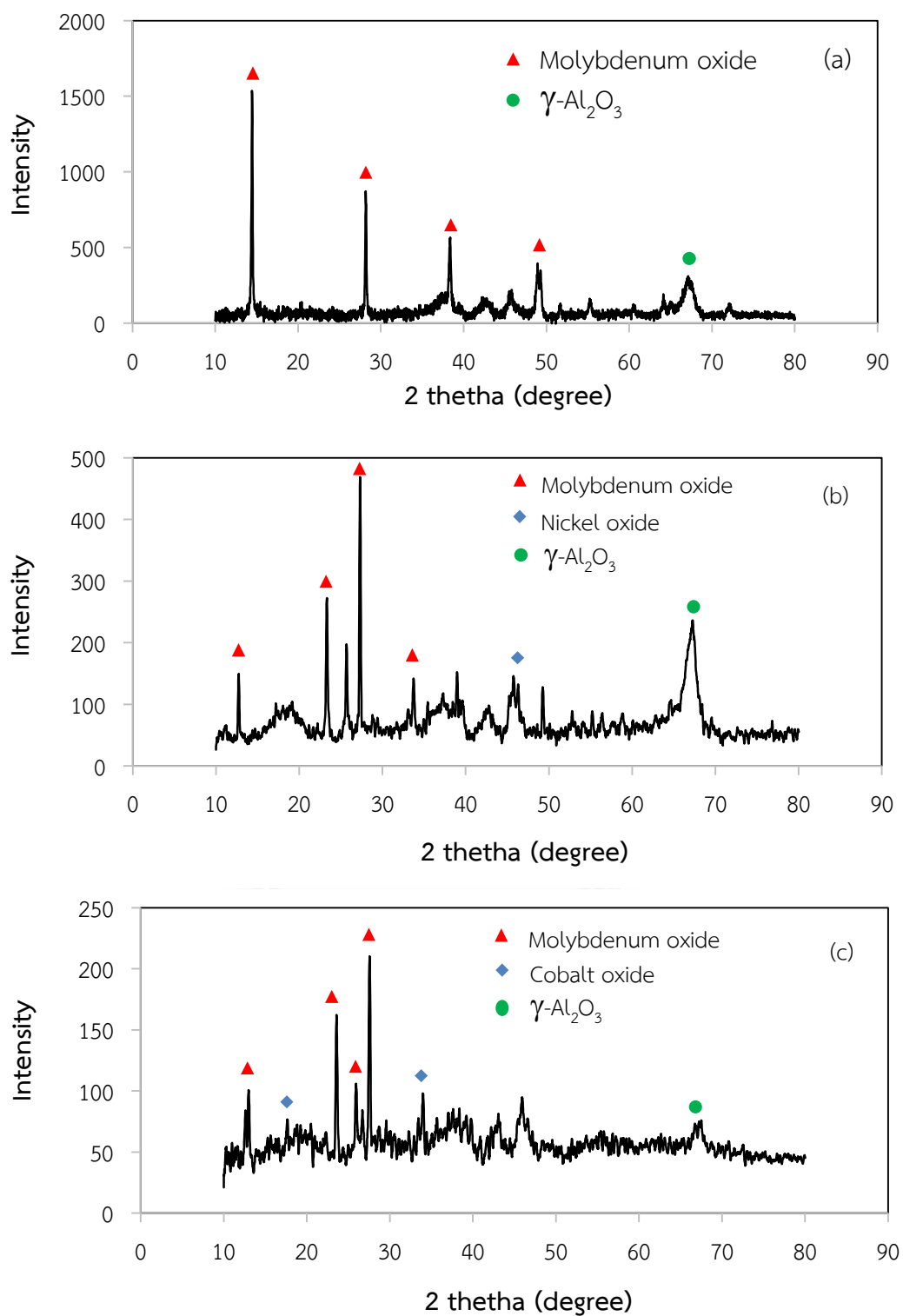


Figure 4.5 XRD patterns of (a) Mo/ γ -Al₂O₃ (b) NiMo/ γ -Al₂O₃ and (c) CoMo/ γ -Al₂O₃ Catalysts.

Normally, the molybdenum sulfide is an active site for the reduction of sulfurous compounds in general crude oils via hydrodesulfurization. The part of sulfur in the Mo-based γ -Al₂O₃ catalyst is converted to H₂S under the H₂ atmosphere and generates the anion vacancy on Mo within the catalyst. The sulfurous compounds in the crude oil will occupy the S²⁻ anion vacancy on Mo to form Mo-S species again. This will release clean hydrocarbons and obtain H₂S as the by-product during hydrodesulfurization process (Wang et al., 2002). To consider the catalysts used in this research, they showed the diffraction peaks of the molybdenum oxide instead of molybdenum sulfide. However, the molybdenum oxide could promote the hydrodesulfurization by converting the oxygen atoms on molybdenum oxide as H₂O under hydrogen atmosphere (Kim et al., 2008). Then, the Mo⁰ state would be released to act as the active sites for hydrodesulfurization.

4.3.4 Temperature Programmed Reduction (TPR)

TPR is a general technique to characterize the reduction ability of metal oxides and their mixtures. It gives a good indication to determine the degree of interaction of NiMo or CoMo supported on the γ -Al₂O₃ (Yu et al., 2008). Moreover, this technique is used to find the most efficient reduction temperature of catalyst before applying to catalyze any reactions. Figure 4.6 showed the TPR profiles of all catalysts used in this research. It was observed that all catalysts contained several well separated reduction peaks. At the low temperature range, the peak could be assigned to the reduction of octahedral Mo species having weak interaction with the γ -Al₂O₃ support. Whereas, the reduction peaks found in the high temperature zone could be assigned as the reduction of tetrahedral Mo species resulted from the strong interaction with the γ -Al₂O₃ support (Ramírez et al., 2000).

The TPR profile of Mo/ γ -Al₂O₃ catalyst shown in Figure 4.6a indicated the three major peaks appearing at 339 °C, 544 °C and 679 °C. The peak at 339 °C was attributed to the reduction of sulfur atoms, which were weak interaction on the catalyst surface. The peaks at 544 °C and 679 °C were attributed to the two reduction steps of MoO₃ species which were lower than those reported in the previous literature. Wang et al. (2012) reported that the TPR profile of MoO₃/ γ -Al₂O₃ catalyst showed the two reduction peaks at 570-760 °C and > 760 °C. The first peaks was assigned to the reduction of octahedrally coordinated Mo⁶⁺ to Mo⁴⁺ (MoO₃ → MoO₂) and the reduction

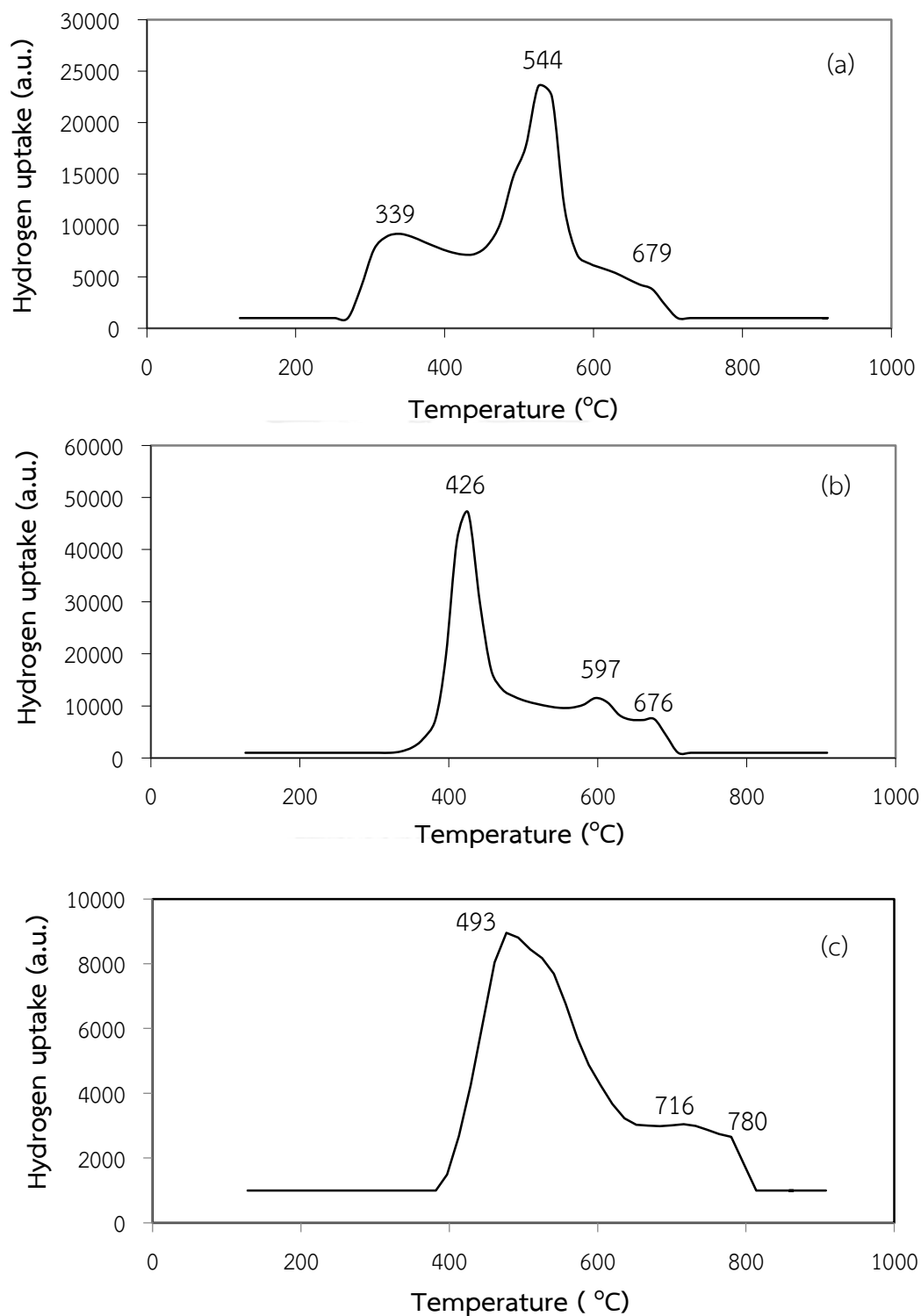


Figure 4.6 TPR Profiles of (a) $\text{Mo}/\gamma\text{-Al}_2\text{O}_3$ (b) $\text{NiMo}/\gamma\text{-Al}_2\text{O}_3$ and (c) $\text{CoMo}/\gamma\text{-Al}_2\text{O}_3$ Catalysts.

of small crystalline MoO_3 . The second peak ($> 760\text{ }^\circ\text{C}$) was assigned as the reduction of Mo^{4+} to Mo^0 ($\text{MoO}_2 \rightarrow \text{Mo}^0$). This could be implied that the $\text{Mo}/\gamma\text{-Al}_2\text{O}_3$ catalyst containing the mixture of MoS_4 and MoO_3 was easier to be reduced at lower temperature.

Figure 4.6b showed the TPR profile of $\text{NiMo}/\gamma\text{-Al}_2\text{O}_3$ catalyst in the range of $100\text{-}900\text{ }^\circ\text{C}$. Three main reduction peaks were observed at 426 , 597 and $676\text{ }^\circ\text{C}$, respectively. The reduction peak at $426\text{ }^\circ\text{C}$ was attributed to the overlap contributions from the reduction of both NiO and NiMoO_4 , while the reduction peaks at 597 and $676\text{ }^\circ\text{C}$ were obtained from the two reduction steps of MoO_3 species ($\text{MoO}_3 \rightarrow \text{MoO}_2 \rightarrow \text{Mo}^0$) (Navarro et al., 2009). The TPR profile of $\text{CoMo}/\gamma\text{-Al}_2\text{O}_3$ catalyst was shown in Figure 4.6c. The three main reduction peaks were observed at 493 , 716 and $780\text{ }^\circ\text{C}$ attributed to the reduction of CoMoO_4 species and the two reduction steps of MoO_3 species, respectively (Navarro et al., 2009).

After the addition of promoters (Co and Ni) onto the $\text{Mo}/\gamma\text{-Al}_2\text{O}_3$ catalyst, the maximum hydrogen consumption peak of TPR profile shifted to the lower temperatures since the promoters decreased the interaction of the metal sulfur bond strength (Raybaud et al., 2000). It was agreed with Figure 4.2 that showed the deposition of promoter at the outer shell of the catalyst and it also related to the standard reduction potentials (E^0) of metals (Mo, Ni and Co). Due to the standard reduction potentials indicated that the tendency for a chemical species to be reduced, which more negative value of E^0 was more easily to be reduced. The E^0 of Mo, Ni and Co were -0.20 , -0.28 and -0.27 V , respectively. Consequently, these catalysts ($\text{NiMo}/\gamma\text{-Al}_2\text{O}_3$ and $\text{CoMo}/\gamma\text{-Al}_2\text{O}_3$) were easier to be reduced under H_2 atmosphere at low temperatures. Therefore, the addition of promoter could enhance the reducibility of Mo (Yoosuk et al., 2008) by promoting the adsorption and dissociation of hydrogen molecules to attack the Mo species and generate coordinative unsaturated site at the edges (Li et al., 2001). The results also showed that the $\text{NiMo}/\gamma\text{-Al}_2\text{O}_3$ catalyst had lower reduced temperature reflecting the easier reduction than $\text{CoMo}/\gamma\text{-Al}_2\text{O}_3$ catalyst due to the stronger interaction of active species with $-\text{OH}$ groups of $\gamma\text{-Al}_2\text{O}_3$ support (Chen et al., 2004). Yu et al. (2008) also found that the lower reduction peak provided the larger amount of active species resulting the higher activity for hydrodesulfurization.

4.3.5 Temperature Programmed Desorption (TPD)

The ammonia temperature programmed desorption is one of the most conventional methods to measure the acidity of catalysts. The amount of ammonia desorbed at a given temperature range is taken to evaluate the acid site concentration, whereas the temperature range at which most of the ammonia is desorbed indicates the acid strength distribution (Benaliouche et al., 2008).

The acidity of the prepared catalysts was analyzed by ammonia TPD. The profiles of ammonia TPD of Mo/ γ -Al₂O₃ catalyst was shown in Figure 4.7a. It indicated that the ammonia desorption profile had two peaks appearing at 235 °C assigned as the desorption of ammonia from the weak acid sites and at 908 °C contributed to the desorption of ammonia from the strong acid sites (Lee et al., 2005). The amount of desorbed ammonia analyzed from the TPD profile of Mo/ γ -Al₂O₃ catalyst was 0.34 mmol/g. From Figure 4.7b, the TPD profile of NiMo/ γ -Al₂O₃ catalyst showed three major peaks appearing at 287 °C for desorption of ammonia from weak acid sites. The other peaks appearing at 752 °C and 907 °C indicated the temperature for ammonia desorption from the stronger acid sites (Lee et al., 2005). The content of adsorbed ammonia evaluated from the TPD profile of NiMo/ γ -Al₂O₃ catalyst was 0.48 mmol/g. For the CoMo/ γ -Al₂O₃ catalyst, Figure 4.7c showed its TPD profile, which was similar to that of NiMo/ γ -Al₂O₃ catalyst. Three major peaks were observed at 279, 486 and 907 °C. The amount of adsorbed ammonia in the TPD profile of CoMo/ γ -Al₂O₃ catalyst was 0.43 mmol/g. The acidity of the catalyst increased in the order of NiMo/ γ -Al₂O₃ > CoMo/ γ -Al₂O₃ > Mo/ γ -Al₂O₃. The increase in the acidity of the catalyst increased the hydrogenation activity and it also simultaneously facilitated the migration of sulfur compounds having methyl groups such as 4,6-dimethyl dibenzothiophene to access the catalyst sites. Thus, the steric hindrance in adsorption of the sulfur compounds on the catalyst surface could be reduced (Kwak et al., 1999).

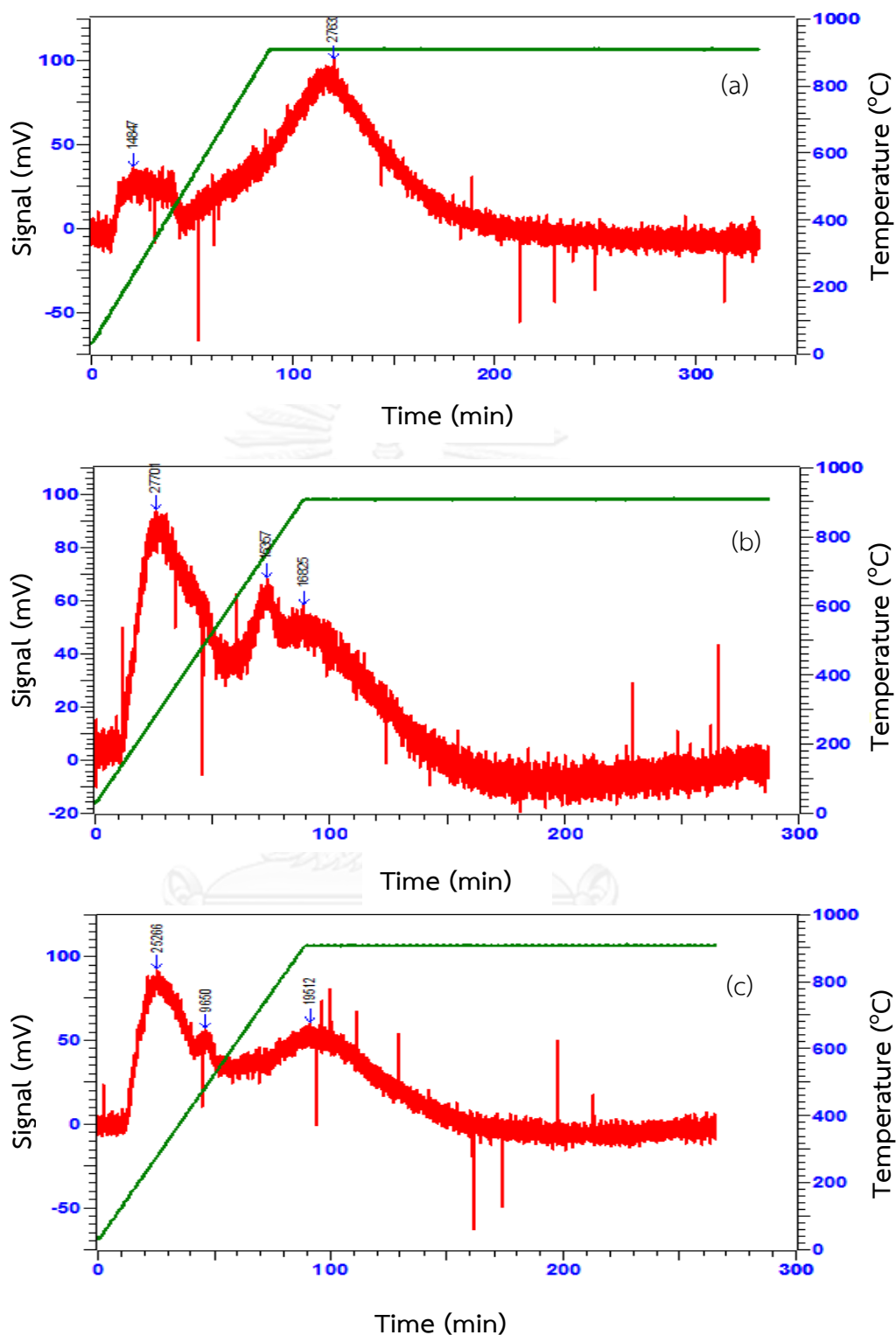


Figure 4.7 TPD Profiles of (a) Mo/ γ -Al₂O₃ (b) NiMo/ γ -Al₂O₃ and (c) CoMo/ γ -Al₂O₃ Catalysts.

4.4 Characterization of Sulfurous Compounds Containing in the Waste Tire Pyrolysis Oil

The appearance of waste tire pyrolysis oil before hydrodesulfurization was shown in Figure 4.8. It was observed that the waste tire pyrolysis oil showed the dark brown color resulted from the color-induced substances, such as unsaturated carbonyl groups, polycyclic aromatic hydrocarbons, quinones, heterocyclic and nitrous compounds (Li et al., 2008).



Figure 4.8 Waste Tire Pyrolysis Oil before Hydrodesulfurization.

To evaluate the amount of sulfurous compounds and briefly classify their species, the waste tire pyrolysis oil before and after hydrodesulfurization was characterized by using GC-FPD. The total GC-FPD area of the waste tire pyrolysis oil before hydrodesulfurization was compared with the total sulfur content value obtained from CHNS-analyzer. Due to the mixture of various sulfurous compounds in the waste tire pyrolysis oil, the sulfurous species in the waste tire oil were categorized as thiophene, benzothiophene and dibenzothiophene derivatives following the standard sulfurous compounds. Figure 4.9a showed the characteristic peaks of GC-FPD for the standard sulfurous compounds: 1.62 min for thiophene, 15.1 min for benzothiophene and 22.2 min for dibenzothiophene. The GC-FPD chromatogram of

waste tire pyrolysis oil shown in Figure 4.9b indicated many peaks with high intensity and high total area at different retention time reflecting the various types and high content of sulfur compounds. From the comparison with the GC-FPD peaks of the sulfurous standard substances (Figure 4.9a), it indicated that the most sulfurous compounds appeared in the waste tire pyrolysis oil were thiophene and benzothiophene derivatives.

From the ultimate analysis of waste tire pyrolysis oil, it showed that the sulfur content in the waste tire pyrolysis oil was 1.15 wt% (Section 4.2) which the %sulfur removal of the waste tire pyrolysis oil after hydrodesulfurization could be calculated from the changing of total peak area of sulfur content analyzed by GC-FPD following Eq. 3.1.

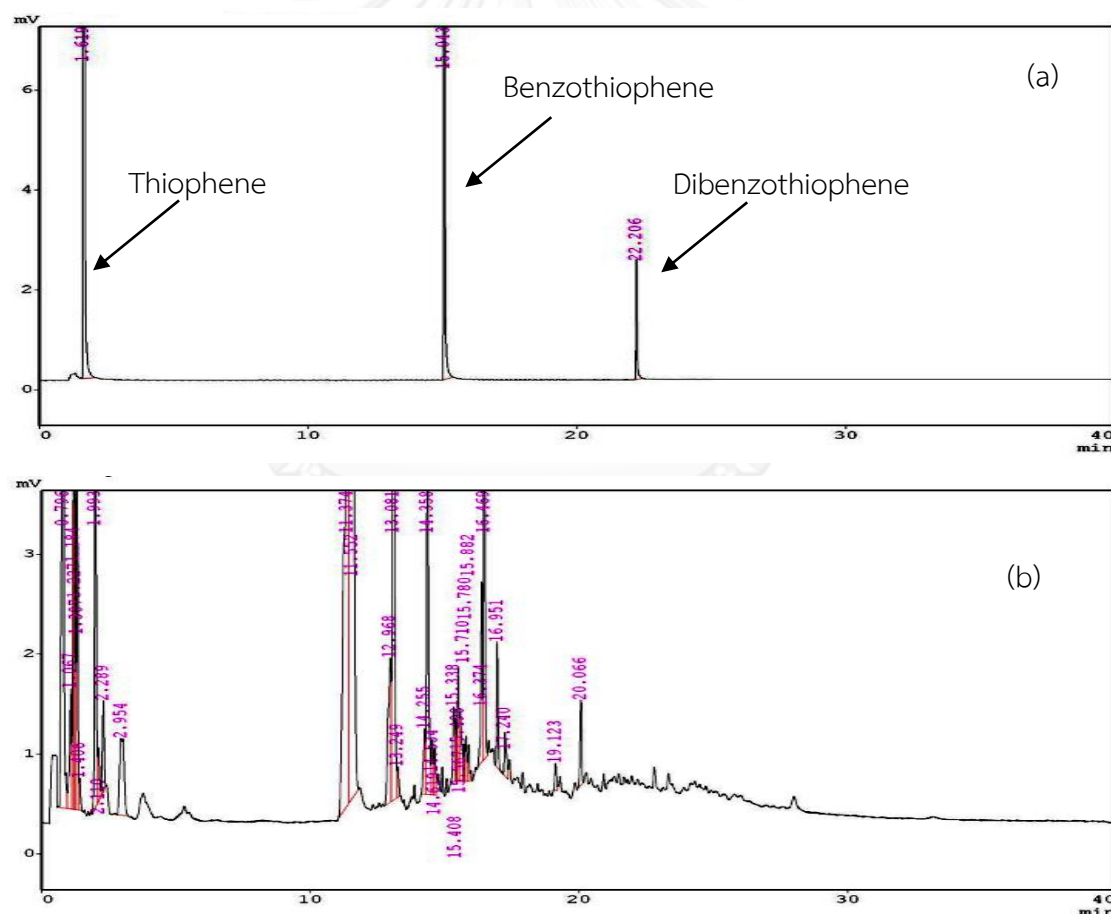


Figure 4.9 GC - FPD Chromatograms of (a) Standard of Sulfurous Compounds (Thiophene, Benzothiophene and Dibenzothiophene) and (b) Waste Tire Pyrolysis Oil.

4.5 Hydrodesulfurization of Waste Tire Pyrolysis Oil

The effect of reaction parameters for catalytic hydrodesulfurization on the efficiency of sulfur removal in the waste tire pyrolysis oil containing sulfur content as 1.15 wt% were investigated using univariate experiment with the center condition as following:

- Catalyst concentration: 0.5 wt% based on the content of waste tire pyrolysis oil dissolved in decane (1/1 (w/w))
- Initial hydrogen pressure: 20 bar
- Reaction temperature: 250 °C
- Reaction time: 30 min

4.5.1 Effect of Catalyst Types and Concentration

The influence of catalyst types and their loading on the sulfur reduction in the waste tire pyrolysis oil was presented in Figure 4.10. The concentration of catalysts were varied from 0-2 wt% based on the content of waste tire pyrolysis oil. Without the addition of catalyst (0 wt% of catalyst concentration), some portion of sulfurous compounds in the waste tire pyrolysis oil (ca. 16%) was eliminated due to the simultaneous thermal hydrodesulfurization and hydrocracking during the reaction (Ramírez et al., 2011). The level of sulfur removal was not high because the aromatic fraction in the waste tire pyrolysis oil was difficult to be converted as smaller ones and it was preferred to agglomerate to form coke (Ramírez et al., 2011).

In the presence of catalysts, the increase in the amount of all catalysts enhanced the level of sulfur removal. When the catalyst concentration increased to 2.0 wt%, the %sulfur removal in the waste tire pyrolysis oil was 87.8, 78.8 and 50.4 wt% for NiMo/ γ -Al₂O₃, CoMo/ γ -Al₂O₃ and Mo/ γ -Al₂O₃ catalysts, respectively. It was found that NiMo/ γ -Al₂O₃ and CoMo/ γ -Al₂O₃ catalysts had higher efficiency to remove sulfur than Mo/ γ -Al₂O₃ catalyst due to the effect of Ni or Co as the promoters to induce the better Mo dispersion on the surface of the catalyst as described in the previous section (Section 4.3.1). Moreover, the addition of promoter also increased the acidity of catalysts, which revealed in TPD technique (Section 4.3.5) leading the higher catalytic activity for hydrodesulfurization (Lee et al., 2005).

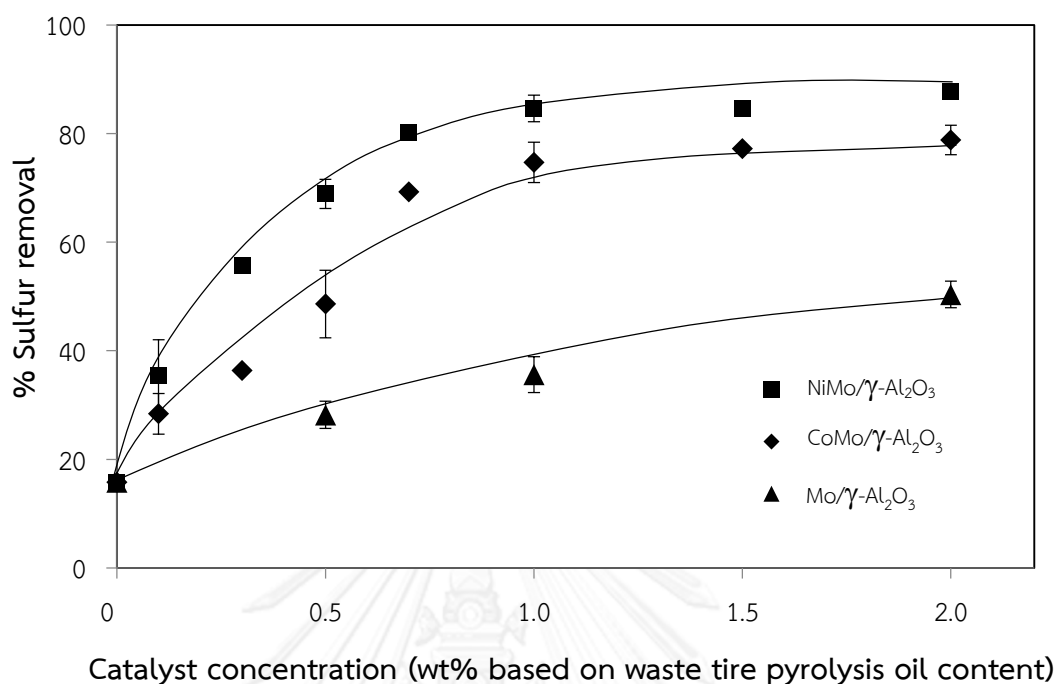


Figure 4.10 Effect of Catalyst Concentration on %Sulfur Removal in the Waste Tire Pyrolysis Oil via Hydrodesulfurization using Mo/ γ -Al₂O₃, CoMo/ γ -Al₂O₃ and NiMo/Al₂O₃ Catalysts (P_{H_2} = 20 bar, T = 250 °C for 30 min).

To consider the effect of Ni and Co promoters for sulfur reduction, the efficiency of CoMo/ γ -Al₂O₃ catalyst for hydrodesulfurization was lower than that of NiMo/ γ -Al₂O₃ catalyst because the physical properties such as surface area, total pore volume and average pore diameter of CoMo/ γ -Al₂O₃ catalyst were lower than those of NiMo/ γ -Al₂O₃ catalyst. Rashidi et al. (2013) reported that the larger pore size could facilitate the diffusion of the large sulfur molecules into the catalyst pores to subsequently interact with the catalytic active species.

The GC-FPD chromatograms of the waste tire pyrolysis oil after hydrodesulfurization catalyzed by Mo/ γ -Al₂O₃, NiMo/ γ -Al₂O₃ and CoMo/ γ -Al₂O₃ catalysts were shown in Figure 4.11a - 4.11c, respectively. They indicated that Mo/ γ -Al₂O₃ catalyst had lowest efficiency to remove sulfur compounds in the waste tire pyrolysis oil. The remaining sulfur compounds in the waste tire

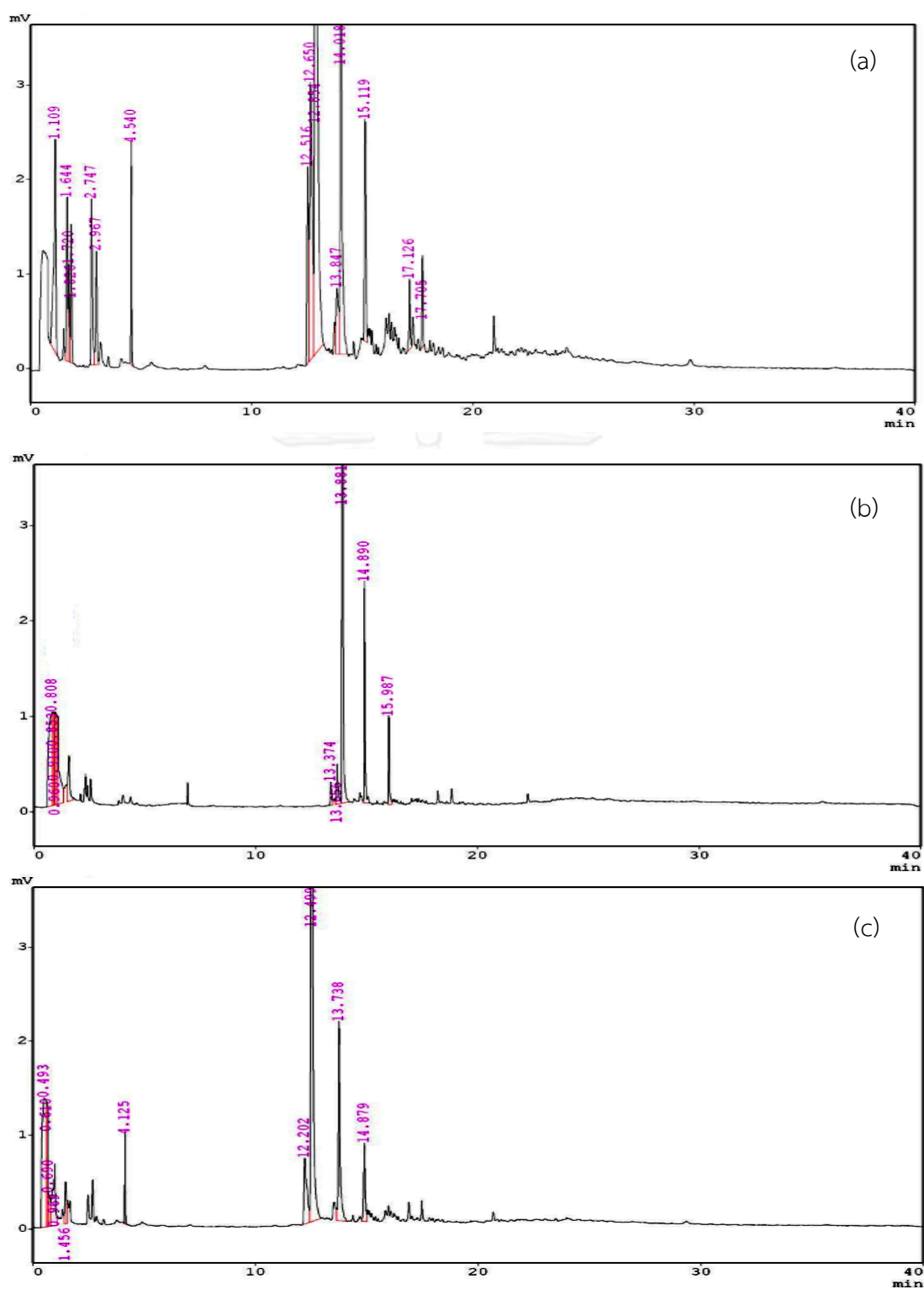


Figure 4.11 GC-FPD Chromatograms of Waste Tire Pyrolysis Oil after Hydrodesulfurization using (a) Mo/ γ -Al₂O₃ (50.4% sulfur removal), (b) NiMo/ γ -Al₂O₃ (87.8% sulfur removal) and (c) CoMo/ γ -Al₂O₃ (78.8% sulfur removal) Catalysts.

pyrolysis oil still had many peaks with high intensity. Whereas, the NiMo/ γ -Al₂O₃ and CoMo/ γ -Al₂O₃ catalysts (Figure 4.11b and Figure 4.11c) showed the higher efficiency to remove sulfurous compounds than the Mo/ γ -Al₂O₃ catalyst. Therefore, the addition of promoter (Ni and Co) into the Mo/ γ -Al₂O₃ catalyst enhanced the activity of the Mo catalyst in the hydrodesulfurization. The NiMo/ γ -Al₂O₃ and CoMo/ γ -Al₂O₃ catalysts increased the hydrogenation and direct desulfurization pathways of the hydrodesulfurization to remove the sulfurous compounds, respectively (Egorova and Prins, 2004). Figure 4.11b and 4.11c also showed that the remaining sulfurous compounds in the waste tire pyrolysis oil might be thiophene and benzothiophene derivatives. It was clearly observed that the peaks appearing in the range of 0-10 min were significantly reduced after hydrodesulfurization implying that thiophene and its derivatives could be significantly reduced due to the formation of Co-Mo-S or Ni-Mo-S active site on the S-edge of MoS₂ which favored the direct desulfurization by the participation of sulfur vacancy (Boukoberine et al., 2011). However, the peak intensity of benzothiophene was more difficult to be reduced by these catalysts possibly since the benzothiophene and its derivatives had many sulfur bonds in aromatic structures, which were difficult to be removed. Moreover, they had alkyl substituents which could induce the steric hindrance to decrease the ability of the substrates to reach the catalytic active sites (Andersson and Schade, 2004).

4.5.2 Effect of Initial Hydrogen Pressure

In hydrodesulfurization, the sulfur compounds in the waste tire pyrolysis oil were removed by converting as H₂S under H₂ atmosphere. Therefore, hydrogen was an important for hydrodesulfurization to provide the multiple roles generation of anion vacancy to remove sulfide, hydrogenation, and hydrogenolysis for sulfur reduction (Moqadam and Mahmoudi, 2013).

The effect of the initial hydrogen pressure on %sulfur removal in the waste tire pyrolysis oil via hydrodesulfurization at 250 °C for 30 min was shown in Figure 4.12. The catalyst concentration was kept constant at 0.5 wt%. The initial hydrogen pressure was varied in the range of 10-50 bar. The results indicated that the higher initial hydrogen pressure increased the sulfur reduction efficiency to eliminate the sulfur compounds in waste tire pyrolysis oil for all applied catalysts in the order of NiMo/ γ -Al₂O₃ > CoMo/ γ -Al₂O₃ > Mo/ γ -Al₂O₃. It could be explained that the increase in the initial hydrogen pressure enhanced the amount of hydrogen in the system to

facilitate the sulfur vacancies on the catalyst active surface by removing sulfur and/or SH groups. These acidic groups were involved in the hydrogenation (HYD) pathway, whereas the sulfur vacancies were related to the direct desulfurization (DDS) pathway for reducing the sulfur compounds (Vogelaar et al., 2003). However, the excessively high initial hydrogen pressure might merely saturate the surface of catalyst to inhibit the access of the sulfurous compounds on the active site (Speight, 1981). The NiMo/ γ -Al₂O₃ catalyst had the highest efficiency to remove sulfur compounds in the waste tire pyrolysis oil to achieve 84.3% sulfur removal. It could be explained that the hydrogen adsorbed on the NiMo/ γ -Al₂O₃ catalyst are unstable and easily captured by any sulfur compounds in the waste tire pyrolysis oil (Badawi et al., 2008). At low initial hydrogen pressure, the CoMo/ γ -Al₂O₃ catalyst had less efficiency to remove the sulfurous compounds than the NiMo/ γ -Al₂O₃ catalyst due to its higher reduction temperature resulting in the more difficulty to be reduced (Section 4.3.4). Thus, the CoMo/ γ -Al₂O₃ catalyst required higher hydrogen pressure to remove the sulfurous compounds at the similar %sulfur removal level as that of the NiMo/ γ -Al₂O₃ catalyst.

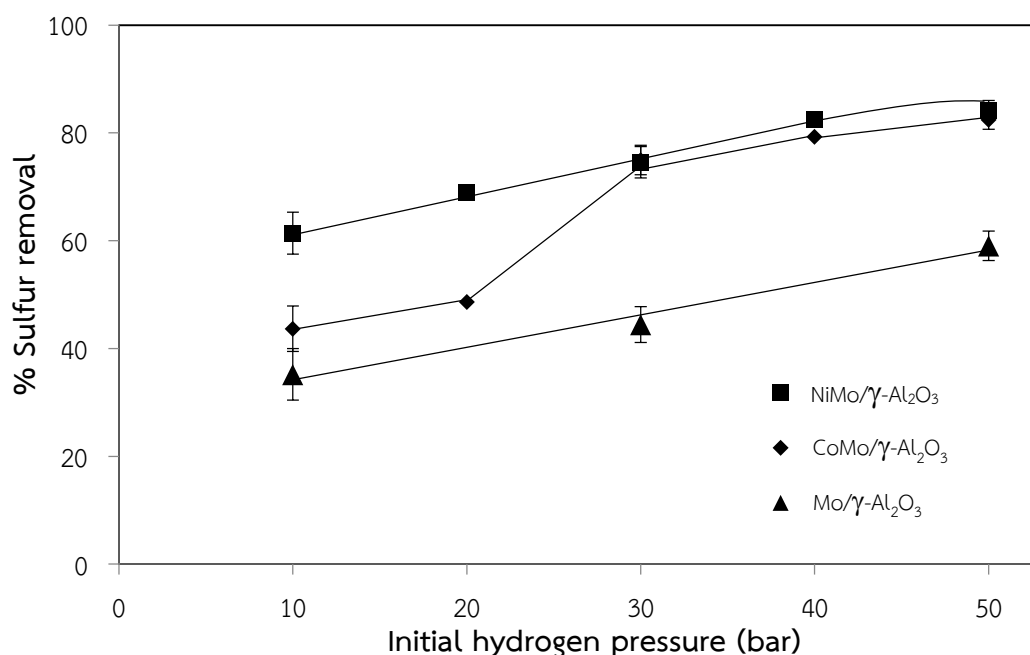


Figure 4.12 Effect of Initial Hydrogen Pressure on %Sulfur Removal in the Waste Tire Pyrolysis Oil via Hydrodesulfurization using Mo/ γ -Al₂O₃, CoMo/ γ -Al₂O₃ and NiMo/ γ -Al₂O₃ Catalysts (Catalyst Concentration = 0.5 wt%, T = 250 °C for 30 min).

4.5.3 Effect of Reaction Temperature

The reaction temperature was an important parameter to affect the catalyst stability and the reaction rate. The effect of the reaction temperature on the hydrodesulfurization performance was investigated in the range of 150-350 °C for 30 min when the catalyst concentration was 0.5 wt%. The results shown in Figure 4.13 indicated that the higher reaction temperature increased the performance of all catalysts to reduce sulfur compounds in the waste tire pyrolysis oil. At 350 °C, it was found that the hydrodesulfurization using NiMo/ γ -Al₂O₃ catalyst provided the maximum %sulfur removal as 84.5%. The results were well supported by the endothermic nature of the hydrodesulfurization reaction, which is favored at high temperature (Yaseen et al., 2012). The high temperatures also increased the rate of proliferation and osmosis of the sulfurous compounds into the pores of the catalyst containing the active sites for hydrodesulfurization (Jarullah et al., 2011). Moreover,

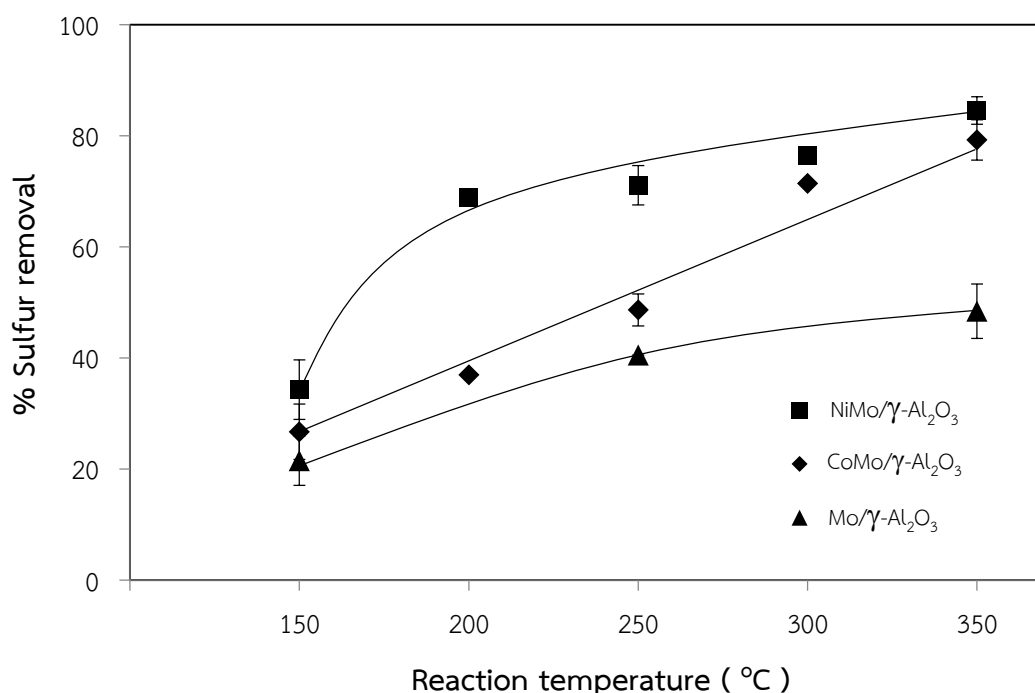


Figure 4. 13 Effect of Reaction Temperature on %Sulfur Removal in the Waste Tire Pyrolysis Oil via Hydrodesulfurization using Mo/ γ -Al₂O₃, CoMo/ γ -Al₂O₃ and NiMo/ γ -Al₂O₃ Catalysts (Catalyst Concentration = 0.5 wt%, P_{H2} = 20 bar for 30 min).

the increase in the reaction temperature could activate the unreactive sulfur compounds, which most properly belonged to thiophene derivatives to react with hydrogen (Mohammed et al., 2008). The higher reaction temperature also decomposed the aromatic compounds as smaller molecules, which were easier to diffuse into the pore of the catalyst (Mohammed et al., 2008). It was clearly observed that NiMo/ γ -Al₂O₃ and CoMo/ γ -Al₂O₃ catalysts had higher efficiency for hydrodesulfurization than Mo/ γ -Al₂O₃ catalyst. It could be described that the addition of Ni and Co as the promoters for Mo/ γ -Al₂O₃ catalyst increased the electron density at the S atom resulting in the enhancement of the activity of H₂ to promote the more S vacancies, which were the catalytic active site (Yoosuk et al., 2008). To compare the efficiency for Ni and Co promoters for Mo catalyst, it was observed that the sulfur removal efficiency of CoMo/ γ -Al₂O₃ catalyst was lower than that of NiMo/ γ -Al₂O₃ catalyst because CoMo/ γ -Al₂O₃ catalyst had stronger interaction between active site and OH⁻ groups of alumina support resulting in the higher difficulty to reduce the anion vacancy on Mo. Thus, the hydrodesulfurization that catalyzed by CoMo/ γ -Al₂O₃ catalyst needed to use the higher reaction temperature (Yu et al., 2008). However, the high reaction temperature might promote the undesirable side reactions such as hydrocracking and thermal cracking, which might affect the properties of the obtained oil (Mohammed et al., 2008).

4.5.4 Effect of Reaction Time

The influence of reaction time on the efficiency of hydrodesulfurization of waste tire pyrolysis oil was presented in Figure 4.14. The hydrodesulfurization proceeded for 5-60 min. The results indicated that the longer reaction time increased the level of sulfur reduction in waste tire pyrolysis oil for all applied catalysts in the order of NiMo/ γ -Al₂O₃ > CoMo/ γ -Al₂O₃ > Mo/ γ -Al₂O₃. This could be explained that the longer reaction time increased the contact time between active sites and sulfurous compounds in the waste tire pyrolysis oil to achieve the better chances for both reforming and HDS reactions (Yaseen et al., 2012).

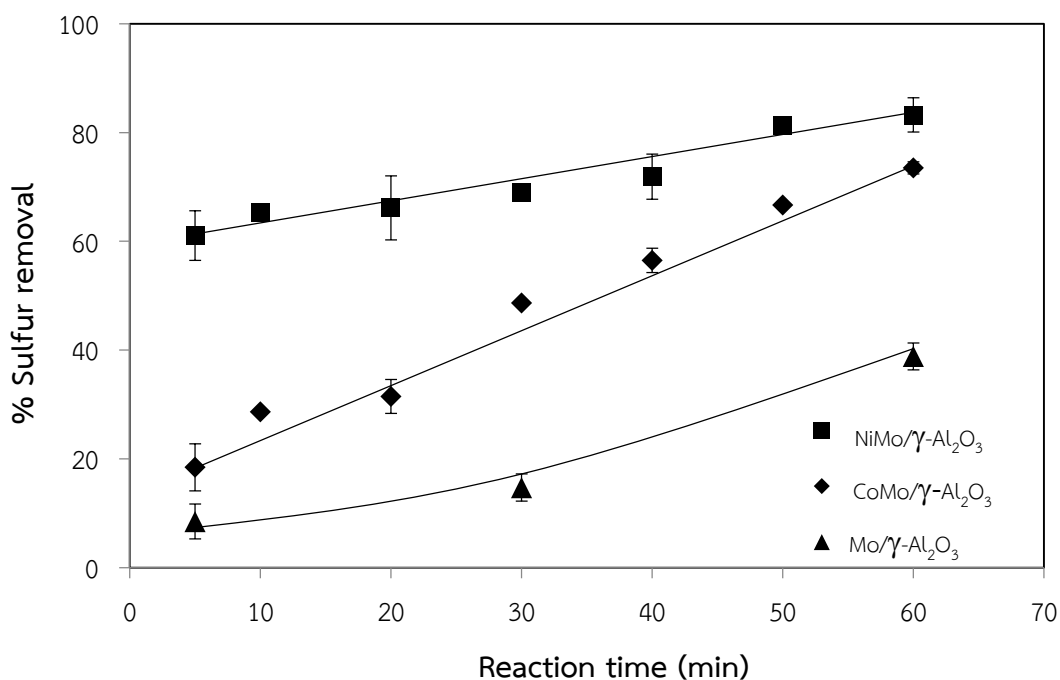


Figure 4.14 Effect of Reaction Time on %Sulfur Removal in the Waste Tire Pyrolysis Oil via Hydrodesulfurization using Mo/ γ -Al₂O₃, CoMo/ γ -Al₂O₃ and NiMo/ γ -Al₂O₃ Catalysts (Catalyst Concentration = 0.5 wt%, P_{H2} = 20 bar, T = 250 °C).

4.6 Quality of Waste Tire Pyrolysis Oil after Hydrodesulfurization

4.6.1 Appearance of Waste Tire Pyrolysis Oil after Hydrodesulfurization

After hydrodesulfurization, the color of waste tire pyrolysis oil was changed from dark brown to visually light yellow as shown in Figure 4.15. It was possible that some color-induced substances such as unsaturated carbonyl groups, polycyclic aromatic hydrocarbons, quinones, heterocyclic and nitrous compounds were eliminated by hydrogenation and/or hydrogenolysis during hydrodesulfurization (Li et al., 2008). This result corresponded with the result of GC-MS which showed that the peaks of color-induced substances were decreased or converted as saturated hydrocarbon.



Figure 4.15 Waste Tire Pyrolysis Oil after Hydrodesulfurization.

4.6.2 Gas Chromatography Simulated Distillation (GC-SIMDIS)

The waste tire pyrolysis oil before and after hydrodesulfurization, diesel and gasoline were analyzed by GC-SIMDIS technique to separate individual hydrocarbon components in the order of their boiling points range. The GC-SIMDIS analysis provided a quantitative percent mass yield as a function of boiling point of the hydrocarbon components in the samples. The hydrocarbon components of waste tire pyrolysis oil before and after hydrodesulfurization, diesel and gasoline were compared with the boiling point range of different fractions as shown in Figure 4.16 and Table 4.6. It indicated that the waste tire pyrolysis oil before and after hydrodesulfurization had the boiling point in the range of 40-450 °C. Before hydrodesulfurization, the waste tire pyrolysis oil was consisted of the light naphtha (41.2 wt%), heavy naphtha (23.3 wt%), atmosphere gas oil (31.0 wt%) and light gas oil (3.5 wt%). After the hydrodesulfurization, the waste tire pyrolysis oil had a lower fraction of heavy naphtha (14.7 wt%), atmosphere gas oil (15.6 wt%) and light gas oil (1.0 wt%) but the light naphtha fraction had higher value as 68.7 wt% due to the

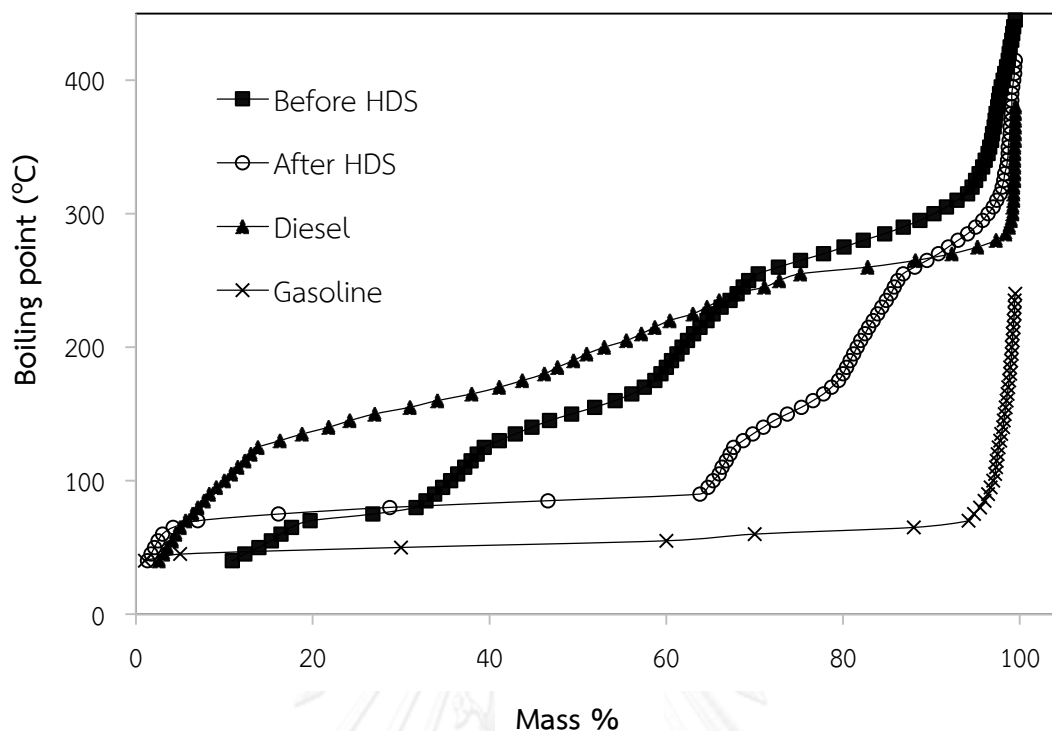


Figure 4.16 GC-SIMDIS chromatograms of Diesel, Gasoline, Waste Tire Pyrolysis Oil before and after Hydrodesulfurization (87.8% sulfur removal).

Table 4.6 %Mass of the Waste Tire Pyrolysis Oil before and after Hydrodesulfurization (Reddy et al., 1998)

Component	Boiling point (°C)	%Mass	
		Before hydrodesulfurization	After hydrodesulfurization
Light naphtha	IBP-130	41.2	68.7
Heavy naphtha	130-220	23.3	14.7
Atmosphere gas oil	220-340	31.0	15.6
Light gas oil	340-450	3.5	1.0
Heavy vacuum gas oil	450-540	-	-
Super heavy gas oil	540-847	-	-
Nondistillable residue	>847	-	-

effect of hydrocracking and thermal cracking of the larger molecules in waste tire pyrolysis oil to be the smaller molecules during hydrodesulfurization. Figure 4.16 also showed the boiling point in the range of 40-380 °C for the diesel and 40-240 °C for the gasoline. To compare the boiling point of diesel and gasoline with the waste tire pyrolysis oil before and after hydrodesulfurization, it was found that the boiling point range of both waste tire pyrolysis oils had similar to that of diesel and gasoline. However, Table 4.6 showed that the waste tire pyrolysis oil after hydrodesulfurization had higher value of light naphtha, which was the main component in gasoline (Tailleur and Albornoz, 2010). Thus, it could be concluded that the waste tire pyrolysis oil after hydrodesulfurization was similar to gasoline-type fuel.

4.6.3 Gas Chromatography/Mass Spectroscopy (GC/MS)

GC/MS technique is consisted of two analytical procedures in sequence, namely a gas chromatography (GC) separation followed by mass spectroscopy (MS) detection. The waste tire pyrolysis oil before and after hydrodesulfurization was analyzed by GC/MS for separation and indication of the types of multiple compounds in the waste tire pyrolysis oil as shown in Figure 4.17 and Table 4.7. Before hydrodesulfurization (Figure 4.17a), the GC/MS chromatogram of the waste tire pyrolysis oil showed the most abundant compounds with high peak area such as cyclopentene (4.78 min), toluene (5.27 min), xylene (8.29 min), benzene (11.8 min) and d-limonene (11.9 min). d-Limonene exhibited the highest peak intensity reflecting the highest concentration. Thus, it was the most important product generated from the pyrolysis of polyisoprene (NR) (UÇar et al., 2005). Limonene was also used in a wide range of industrial applications such as solvents, resins, adhesives and a feedstock for the production of flavorings and fragrances (Hayworth et al., 1995). Moreover, the GC/MS chromatogram of the waste tire pyrolysis oil before hydrodesulfurization showed the oxygenated compounds such as cyclohexanol (8.33 min) and benzenepropanoic acid (8.87 min) etc., obtained from the thermal degradation of some oxygenated substances in the waste tire, such as stearic acid, extender oils etc., (Laresgoiti et al., 2004). The nitrogenated and sulfurated compounds were also found in the waste tire pyrolysis oil such as benzothiazole (15.38 min), which was derived from the decomposition of accelerators used in tire compounding (Laresgoiti et al., 2004).

Figure 4.17b showed the GC/MS chromatogram of the waste tire pyrolysis oil after hydrodesulfurization. To compare with the GC/MS chromatogram of waste tire pyrolysis oil before treating as shown in Figure 4.17a, it was found that the peak intensity of the most peaks appeared in the waste tire pyrolysis oil decreased after hydrodesulfurization; especially, xylene, benzenepropanoic acid, d-limonene and benzothiazole. Whereas some peak was disappeared after hydrodesulfurization such as cyclopentene and toluene.

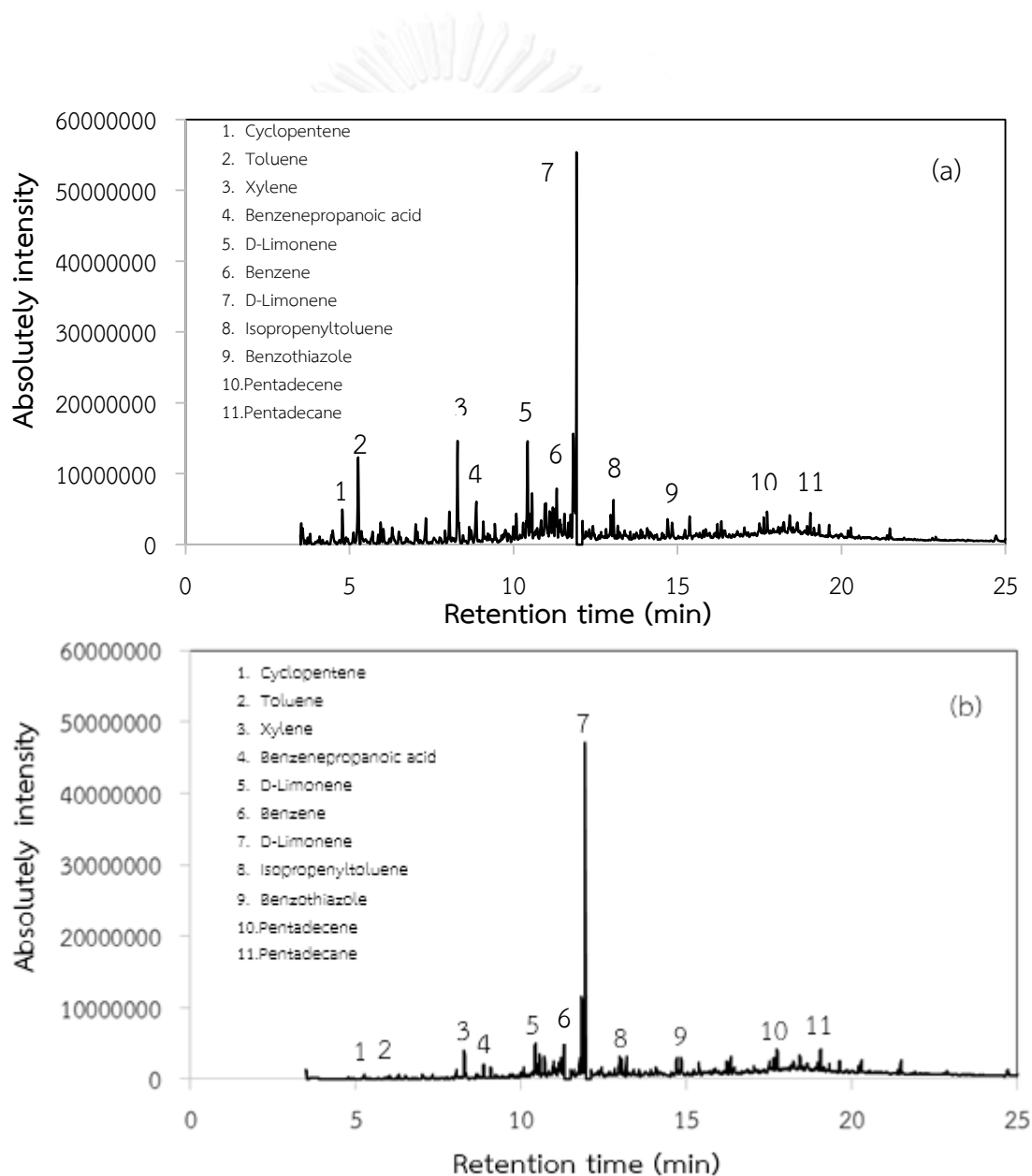


Figure 4.17 GC/MS Chromatograms of Waste Tire Pyrolysis Oil (a) before and (b) after Hydrodesulfurization.

Table 4.7 Tentative GC/MS Characterization of Waste Tire Pyrolysis Oil

Peak number	Retention time (min)	Tentative assignment	Peak area	
			Before HDS	After HDS
1	4.78	Cyclopentene	4,959,177	N/A
2	5.27	Toluene	12,287,659	N/A
3	8.29	Xylene	14,646,154	4,090,277
4	8.87	Benzenepropanoic acid	6,026,243	1,917,681
5	10.43	D-Limonene	14,592,976	5,091,804
6	11.83	Benzene	15,639,779	8,833,640
7	11.93	D-Limonene	55,365,663	32,938,637
8	13.05	Isopropenyltoluene	6,292,813	2,211,451
9	15.38	Benzothiazole	3,967,738	2,395,181
10	17.63	Pentadecene	3,853,352	2,959,790
11	19.05	Pentadecane	4,478,605	4,183,629

4.6.4 Viscosity, Copper Strip Corrosion, Heating Value and Iodine Value

Table 4.8 showed the quality of waste tire pyrolysis oil after hydrodesulfurization and compared to diesel and gasoline such as heating value (ASTM D 2015), viscosity (ASTM D445) and corrosive property (ASTM D 130). The results showed the heating value of waste tire pyrolysis oil after hydrodesulfurization was 44 MJ/kg which was higher than that of waste tire oil before hydrodesulfurization (42 MJ/kg). This means that this process was slightly increased the heating value of waste tire pyrolysis oil. Moreover, the heating value of waste tire pyrolysis oil after hydrodesulfurization was also close to that of diesel (45 MJ/kg) and gasoline (47 MJ/kg). Thus, it was possible to totally or partially replace the conventional liquid fuels with hydrodesulfurized waste tire pyrolysis oil.

Table 4.8 Viscosity, Copper Strip Corrosion, Heating Value and Iodine Value of Oils

Products	Heating value (MJ/kg)	Viscosity (cSt)	Copper strip corrosion	Iodine value (g I ₂ /100 g)
Diesel	45.0	2.0-5.0 ^a	Not worse than No.1 ^a	14.6
Gasoline	47.0	0.53 ^a	Not more than No.1 ^a	14.6
Waste tire pyrolysis oil before hydrodesulfurization	42.0	3.90	Not change	108
Waste tire pyrolysis oil after hydrodesulfurization (87.8 % sulfur removal)	44.0	3.45	Not change	95.0

^a Standard for diesel and gasoline quality (USEPA, 1996)

After hydrodesulfurization, the viscosity of waste tire pyrolysis oil (3.45 cSt.) was slightly lower than that of waste tire pyrolysis oil before hydrodesulfurization (3.90 cSt.) possibly due to the increase in the rate of hydrogenation and hydrocracking leading the chain scission and breaking bond of sulfurous compounds during hydrodesulfurization (Mohammed et al., 2008). The results indicated that the viscosity of waste tire pyrolysis oil before and after desulfurization was in the range of viscosity of the commercial diesel (2.0-5.0 cSt.), but it was higher than the gasoline fuel (0.53 cSt.).

From the test of the copper strip corrosion, the result showed that the waste tire pyrolysis oil before and after hydrodesulfurization did not change the color of copper strip. This indicated that the waste tire pyrolysis oil did not have the corrosive property and thus it could be applied for equipments made from copper. Moreover, the iodine value of waste tire pyrolysis oil before and after hydrodesulfurization were 108 and 95.0 (g I₂/100 g), respectively. This result exhibited that the waste tire pyrolysis oil after hydrodesulfurization had higher saturation, which corresponded with the result of the GC/MS analysis (Section 4.7.3) that showed the peak intensity of the unsaturation compounds in the waste tire pyrolysis oil were decreased after hydrodesulfurization.

This result induced the color of waste tire pyrolysis oil was shifted from dark brown to visually light yellow as shown in Figure 4.16. However, the iodine value of waste tire pyrolysis oil was higher than the diesel and gasoline (14.6 g I₂/100 g), which adversely affecting the fuel properties such as increasing viscosity, poor combustion, high emissions and engine failure (Jahirul et al., 2013). This implied that some unsaturated compounds still existed in the hydrodesulfurized waste tire pyrolysis oil.



CHAPTER V

CONCLUSIONS

5.1 Conclusions

This research work aimed to reduce the sulfur content in the alternative liquid fuel derived from pyrolysis of waste tire pyrolysis via hydrodesulfurization catalyzed by using molybdenum supported on γ -alumina ($\text{Mo}/\gamma\text{-Al}_2\text{O}_3$), nickel-molybdenum supported on γ -alumina ($\text{NiMo}/\gamma\text{-Al}_2\text{O}_3$) and cobalt-molybdenum supported on γ -alumina ($\text{CoMo}/\gamma\text{-Al}_2\text{O}_3$). The effect of reaction parameters: catalyst concentration, initial hydrogen pressure, reaction temperature and reaction time on the %sulfur removal was investigated and the kinetics of hydrodesulfurization was also studied. The results of this research work can be summarized as follows:

5.1.1 Characterization of Waste Tire and Its Pyrolysis Products

The waste tire powder had a large content of volatile matter (57.5 wt%) with low moisture content (0.80 wt%). Moreover, the waste tire powder also had high heating value (32.3 MJ/kg). However, the waste tire powder also contained a large amount of sulfurous compounds (1.53 wt%) obtained from vulcanization for tire production. The waste tire powder had the decomposition temperature in a range from 200 to 500 °C and the maximum decomposition temperature about 370 °C. After pyrolysis of waste tire powder, the product yields were consisted of condensed oil, residual oil, char and gas fractions at a composition of 42.0, 4.0, 41.6 and 12.4 wt%, respectively. Since the condensed oil was the highest fraction, it was the most practicability to be scaled up than the residual one. Thus, it was selected as the raw material for upgrading via hydrodesulfurization. The condensed oil had heating value as 42 MJ/kg with 1.15 wt% of sulfur content.

5.1.2 Catalysts Characterization

The Mo/ γ -Al₂O₃, NiMo/ γ -Al₂O₃ and CoMo/ γ -Al₂O₃ catalysts prepared by successive incipient wetness impregnation method had different properties and different hydrodesulfurization performance. For BET surface area, Mo/ γ -Al₂O₃ showed high surface area (96.03 m²/g). The addition of promoters (Ni and Co), significantly decreased the surface area and pore volume of catalysts. From SEM analysis, the addition of promoters led to the improvement of the dispersion of catalytically active Mo species. For the elemental analysis by EDX, NiMo/ γ -Al₂O₃ had the highest Mo content as 9 wt% corresponding to the result of Mo mapping. It made NiMo/ γ -Al₂O₃ had higher amount of active sites. XRD results showed that the different crystalline of metal oxides were depended on the promoter applied in the catalyst. The addition of promoter induced low peak intensity of crystalline of molybdenum oxide. The result from TPR analysis showed that the addition of promoters to the Mo/ γ -Al₂O₃ caused a significant downward shift of the peak reduction temperature suggesting the lower metal sulfur bond energy. Consequently, the NiMo/ γ -Al₂O₃ catalyst was slightly easier to be reduced. The acidity of the catalyst analyzed by ammonia TPD indicated that NiMo/ γ -Al₂O₃ catalyst had higher acidity than Mo/ γ -Al₂O₃ and CoMo/ γ -Al₂O₃.

5.1.3 Hydrodesulfurization of Waste Tire Pyrolysis Oil

The increase in the catalyst concentration, reaction temperature, reaction time and initial hydrogen pressure enhanced the performance of hydrodesulfurization to reduce sulfurous compounds in the waste tire pyrolysis oil. The maximum %sulfur removal was 87.8 wt% when 2 wt% catalyst concentration of NiMo/ γ -Al₂O₃ was loaded into the system at the center condition (P_{H2} = 20 bar, T = 250 °C for 30 min). The hydrodesulfurization of waste tire pyrolysis oil confirmed that the addition of Ni or Co as the catalyst promoters significantly increased the catalytic activity. It was also found that NiMo/ γ -Al₂O₃ was more active than CoMo/ γ -Al₂O₃ catalyst. Thus, the sulfur content of each fraction could be concluded as follows: waste tire powder (1.53 wt%) → condensed oil (1.15 wt%) → hydrodesulfurized oil (0.14 wt%).

The waste tire pyrolysis oil before and after hydrodesulfurization was characterized by using GC-FPD to evaluate the type and amount of sulfurous compounds. The results indicated that the waste tire pyrolysis oil before hydrodesulfurization had various types and high content of sulfurous compounds. The most sulfur compounds were thiophene, benzothiophene, dibenzothiophene and others with smaller molecules. After hydrodesulfurization, the sulfurous compounds in waste tire pyrolysis oil were reduced; especially, thiophene and its derivatives.

5.14 Quality of Waste Tire Pyrolysis Oil after Hydrodesulfurization

The heating value of waste tire pyrolysis oil after hydrodesulfurization was slightly higher than that of waste tire pyrolysis oil before hydrodesulfurization and close to that of diesel and gasoline. The viscosity of the waste tire pyrolysis oil was in the range of viscosity of the diesel and higher than the gasoline. Moreover, the waste tire pyrolysis oil did not have the corrosive property and it was also higher saturation. Thus, the waste tire pyrolysis oil after hydrodesulfurization had high potential to totally or partially replace the conventional fossil liquid fuels.

5.2 Recommendations

Since the sulfur content in the hydrodesulfurized waste tire pyrolysis oil obtained from the best condition is still over the standard limitation, another process should be added to enhanced the system performance to reduce the sulfur content in the waste tire pyrolysis oil such as the addition of some adsorbents with appropriate pore size to reduce the amount of sulfur compounds remaining in the hydrodesulfurized waste tire pyrolysis oil. The deep hydrodesulfurization is also recommended to achieve the higher efficiency to remove the sulfur compounds in the waste tire pyrolysis oil.

REFERENCES

- Al-Zeghayer, Y. S., and Jibril, B.Y. (2006). Kinetics of hydrodesulfurization of dibenzothiophene on sulfide commercial Co-Mo/ γ -Al₂O₃ catalyst. The Journal of Engineering Research 3: 38-42.
- Amari, T., Themelis, N.J., and Wernick, I.K. (1999). Resource recovery from used rubber tires. Resources Policy 25: 179-188.
- Andersson, J. T., and Schade, T. (2004). Higher alkylated dibenzothiophenes in some crude oils and hydrodesulfurized fuels. Fuel Chemistry 49: 338.
- Anpo, M., Kamat, P.V.V. (2010). Environmentally Benign Photocatalysts: Applications of Titanium Oxide-based Materials. New York, U.S.A. : Springer.
- Badawi, M., Vivier, L., Pérot, G., and Duprez, D. (2008). Promoting effect of cobalt and nickel on the activity of hydrotreating catalysts in hydrogenation and isomerization of olefins. Journal of Molecular Catalysis A : Chemical 293: 53-58.
- Chang, Y. M. (1996). On pyrolysis of waste tire: degradation rate and product yields. Resources, Conservation and Recycling 17: 125-139.
- Chen, H., Zhou, X., Shang, H., Liu, C., Qiu, J., and Wei, F. (2004). Study of dibenzothiophene adsorption over carbon nanotube supported CoMo HDS catalysts. Journal of Natural Gas Chemistry 13: 209-217.
- Choi, G. G., Jung, S.H., Oh, S.J., and Kim, J.S. (2014). Total utilization of waste tire rubber through pyrolysis to obtain oils and CO₂ activation of pyrolysis char. Fuel Processing Technology 123: 57-64.
- Dai, X., Yin, X., Wu, C., Zhang, W., and Chen, Y. (2001). Pyrolysis of waste tires in a circulating fluidized-bed reactor. Energy 26: 385-399.
- Datta, R. N. (2001). Rubber Curing Systems. Shropshire, United Kingdom: Rapra Technology.
- Deng, Z., Wang, T., and Wang Z. (2010). Hydrodesulfurization of diesel in a slurry reactor. Chemical Engineering Science 65: 480-486.
- Dickey, P. A. (1981). Petroleum Development Geology. English: PennWell Corporation.

- Egorova, M., and Prins, R. (2004). Hydrodesulfurization of dibenzothiophene and 4,6-dimethyldibenzothiophene over sulfide NiMo/ γ -Al₂O₃, CoMo/ γ -Al₂O₃, and Mo/ γ -Al₂O₃ catalysts. Journal of Catalysis 225: 417-427.
- Galvagno, S., Casu, S., Casabianca, T., Calabrese, A., and Cornacchia, G. (2002). Pyrolysis process for the treatment of scrap tyres: preliminary experimental results. Waste Management 23: 917-923.
- Gregg, S. J., and Sing, K.S.W. (1967). Adsorption Surface Area and Porosity. London: Academic Press.
- Gutiérrez, O. Y., Valencia, D., Fuentes, G.A., and Klimova, T. (2007). Mo and NiMo catalysts supported on SBA-15 modified by grafted ZrO₂ species: Synthesis, characterization and evaluation in 4,6-dimethyldibenzothiophene hydrodesulfurization. Journal of Catalysis 249: 140-153.
- Hamed, G. R. (1992). Engineering with Rubber How to Design Rubber Components. Munich: Hanser.
- Hayworth, J. E., Burrell, T., Olson, J., and Hanson, C.D. (1995). A New Pyrolysis Reactor for Increased Limonene Yield in Scrap Tire Pyrolysis. Iowa: Department of Chemistry, University of Northern Iowa.
- Hertz, D. L. (1984). Elastomerics. U.S.A: A Publication of Communication Channels, Inc.
- Islam, M. R., Islam, M.N., Mustafi, N.N., Rahim, M.A., and Haniu, H. (2013). Thermal recycling of solid tire wastes for alternative liquid fuel: the first commercial step in Bangladesh. Procedia Engineering 56: 573-582.
- Jahirul, M. I., Brown, R.J., Senadeera, W., O'Hara, I.M. and Ristovski, Z.D. (2013). The use of artificial neural networks for identifying sustainable biodiesel feedstocks. Energies 6: 3764-3806.
- Jarullah, A. T., Mujtaba, I.M., and Wood, A.S. (2011). Kinetic parameter estimation and simulation of trickle-bed reactor for hydrodesulfurization of crude oil. Chemical Engineering Science 66: 859-871.
- Juma, M., Korenova, Z., Markos, J., Annus, J., and Jelemensky, L. (2006). Pyrolysis and combustion of scrap tire. Petroleum and Coal 48: 15-26.

- Khodadadi, A., Angaji, M.T., Rafsanjani, A.T., and Yonesi, A. (2012). Adsorptive desulfurization of diesel fuel with nano copper oxide (CuO). Proceedings of the 4th International Conference on Nanostructures (ICNS4), pp. 1197-1199. Kish Island: Iran.
- Kim, B. S., Kim, E.Y., Jeon, H.S., Lee, H.I., and Lee, J.C. (2008). Study on the reduction of molybdenum dioxide by hydrogen. Materials Transactions 49: 2147-2152.
- Kowsari, E. (2013). Recent advances in the science and Technology of desulfurization of diesel fuel using ionic liquids. Croatia: Intech.
- Kwak, C., Kim, M.Y., Choi, K., and Moon, S.H. (1999). Effect of phosphorus addition on the behavior of CoMoS/Al₂O₃ catalyst in hydrodesulfurization of dibenzothiophene and 4,6-dimethyldibenzothiophene. Applied Catalysis A: General 185: 19-27.
- Lamonier, C., Soogund, D., Mazurelle, J., Blanchard, P., Guillaume, D., and Payen, E. (2005). Origin of the dispersion limit in the preparation of Ni(Co)Mo/Al₂O₃ and Ni(Co)Mo/TiO₂ HDS oxidic precursors. Scientific Bases for the Preparation of Heterogeneous Catalysts: 713-720.
- Laresgoiti, M. F., Caballero, B.M., Marco, I., Torres, A., Cabrero, M.A., and Chomon, M.J. (2004). Characterization of the liquid products obtained in tyre pyrolysis. Journal of Analytical and Applied Pyrolysis 71: 917-934.
- Lee, J. J., Kim, H., Koh, J.H., Jo, A., and Moon, S.H. (2005). Performance of fluorine-added CoMo₅/Al₂O₃ prepared by sonochemical and chemical vapor deposition methods in the hydrodesulfurization of dibenzothiophene and 4,6-dimethyldibenzothiophene. Applied Catalysis B: Environmental 61: 274-280.
- Li, J., Wang, C., and Yang, Z. (2008). Decolorization of biopetroleum and analysis of colored components. Industrial & Engineering Chemistry Research 47: 4924-4928.
- Li, Y. W., Pang, X.Y., and Delmon, B. (2001). Role of hydrogen in HDS/HYD catalysis over MoS₂: an ab initio investigation. Journal of Molecular Catalysis A: Chemical 169: 259-268.

- Ma, X., Sun, M.L., and Song, C. (2002). A new approach to deep desulfurization of gasoline, diesel fuel and jet fuel by selective adsorption for ultra-clean fuels and for fuel cell applications. Catalysis Today 77: 107-116.
- Martinez, J. D., Puy, N., Murillo, R., Garcia, T., Navarro, M.V., and Mastral, A.M. (2013). Waste tyre pyrolysis – A review. Renewable and Sustainable Energy Reviews 23: 179-213.
- Matar, S., and Hatch, L.F. (1994). Chemistry of Petrochemical Processes. Houston, Texas: Gulf Publishing Company.
- Mohammed, A. H. A. K., Karim, A.M.A., and Areff, H.A. (2008). Effect of operating conditions on hydrodesulfurization of vacuum gas oil. Iraqi Journal of Chemical and Petroleum Engineering 9: 57-67.
- Moqadam, S. I., and Mahmoudi, M. (2013). Advent of nanocatalysts in hydrotreating process: benefits and developments. American Journal of Oil and chemical Technologies 1: 13-21.
- Moses, P. G., and Hinnemann, B., Topsoe, H., and Norskov, J.K. (2009). The effect of Co-promotion on MoS₂ catalysts for hydrodesulfurization of thiophene: A density functional study. Journal of Catalysis 268: 201-208.
- Natarajan, E., Nordin, A., and Rao, A.N. (1998). Overview of combustion and gasification of rice husk in fluidized bed reactors. Biomass Bioenergy 14: 533-546.
- Navarro, R. M., Castano, P., Alvarez-Galvan, M.C., and Pawelec, B. (2009). Hydrodesulfurization of dibenzothiophene and a SRGO on sulfide Ni(Co)Mo/Al₂O₃ catalysts. Effect of Ru and Pd promotion. Catalysis Today 143: 108-114.
- Nijhuis, T. A., Koten, G.V., Kapteijn, F., and Moulijn, J.A. (2003). Separation of kinetics and mass-transport effects for a fast reaction: the selective hydrogenation of functionalized alkynes. Catalysis Today 79-80: 315-321.
- Niyogi, U. K. (2007). Polymer Additives and Compounding [Online], Available from: <http://www.scribd.com/doc/142526912/Revised-Additives-for-Rubber.html>, [2013,May 17].
- öner, C., and Altun, S. (2009). Biodiesel production from inedible animal tallow and an experimental investigation of its use as alternative fuel in a direct injection diesel engine. Applied Energy 86: 2114-2120.

- Orza, R. (2008). Investigation of peroxide crosslinking of EPDM rubber by solid-state NMR. Eindhoven, Netherland: Technische Universiteit Eindhoven.
- Ramirez, J., Contreras, R., Castillo, P., Klimova, T., Zarate, R., and Luna, R. (2000). Characterization and catalytic activity of CoMo HDS catalysts supported on alumina-MCM-41. Applied Catalysis A: General 197: 69-78.
- Ramirez, S., Ancheyta, J., Centeno, G., and Marroquin, G. (2011). Non-catalytic hydrodesulfurization and hydrodemetallization of residua. Fuel 90: 3571-3576.
- Rashidi, F., Sasaki, T., Rashidi, A.M., Kharat, A.N., and Jozani, K.J. (2013). Ultradeep hydrodesulfurization of diesel fuels using highly efficient nanoalumina-supported catalysts: Impact of support, phosphorus, and/or boron on the structure and catalytic activity. Journal of Catalysis 299: 321-335.
- Rattanasupa, B. (2007). The development of rubber compound based on NR and EPDM for Playground rubber Mat. Master's Thesis, Department of Chemistry, Faculty of Science, Kasetsart University.
- Raybaud, P., Hafner, J., Kresse, G., Kasztelan, S., and toulhoat, H. (2000). Structure, energetics, and electronic properties of the surface of a promoted MoS₂ catalyst: An ab initio local density functional study. Journal of Catalysts 190: 128-143.
- Reddy, K. M., Wei, B., and Song, C. (1998). High-temperature simulated distillation GC analysis of petroleum resids and their products from catalytic upgrading over Co-Mo/Al₂O₃ catalyst. Catalysis Today 43: 187-202.
- Rinaldi, N., Kubota, T., and Okamoto, Y. (2010). Effect of citric acid addition on the hydrodesulfurization activity of MoO₃/Al₂O₃ catalysts. Applied Catalysis A: General 374: 228-236.
- Rodgers, B., and Waddell, W. (2013). Tire Engineering. Texas, U.S.A.: Elsevier Inc.
- Speight, J. G. (1981). The desulfurization of heavy oils and residua. New York, U.S.A.: Marcel Dekker Inc.
- Tailleur, R. G., and Alborno, C. (2010). Simulation of light naphtha dimerization using a PtZrGa/Si mesoporous catalyst in a swing mode of operation. Catalysis Today 150: 308-318.

- Tavasoli, A., Karimi, S., Zolfaghari, Z., Taghavi, S., Amirfirouzkouhi, H., and Babatabar, M. (2013). Cobalt loading effects on the physic-chemical properties and performance of Co promoted alkalized MoS₂/CNTs catalysts for higher alcohols synthesis. Iran Journal Chemistry Chemical Engineering 32: 21-29.
- Trakarnpruk, W., Seentrakoon, B., and Porntangjitlikit, S. (2008). Hydrodesulfurization of diesel oils by MoS₂ catalyst prepared by in situ decomposition of ammonium thiomolybdate, Silpakorn University Science and Technology Journal, pp. 7-13. Nakornpathom: Silpakorn University.
- Ucar, S., Karagoz, S., Ozkan, A.R., and Yanik, J. (2005). Evaluation of two different scrap tires as hydrocarbon source by pyrolysis. Fuel 84: 1884-1892.
- Vijaya, S., Chow, M.C., and Ma, A.N. (2004). Energy database of the oil palm. MPOB Palm Oil Engineering Bulletin 70: 15-22.
- Vogelaar, B. M., Kagami, N., Langeveld, A.D.V., Eijsbouts, S., and Moulijn, J.A. (2003). Active sites and activity in HDS catalysis: the effect of H₂ and H₂S partial pressure. Preprints of Papers-American Chemical Society, Division of Fuel Chemistry 48(2): 548-549.
- Walsh, M. P. (2006). How to reduce air pollution with cleaner fuels and cleaner vehicles [Online], Available from: <http://www.walshcarlines.com/pdf/Cleaner%20Fuels%20and%20Cleaner%20Vehicle%20UN%20CSD.pdf> , [2013,June 1].
- Wang, B., Ding, G., Shang, Y., Lv, J., Wang, H., Wang, E., Li, Z., Ma, X., Qin, S., and Sun, Q. (2012). Effects of MoO₃ loading and calcination temperature on the activity of the sulphur-resistant methanation catalyst MoO₃/γ-Al₂O₃. Applied Catalysis A: General 431-432: 144-150.
- Wang, C. H., Tsai, T.C., and Wang, I. (2009). Deep hydrodesulfurization over Co/Mo catalysts supported on oxides containing vanadium. Journal of Catalysis 262: 206-214.
- Wang, D., Qian, W., Ishihara, A., and Kabe, T. (2002). Elucidation of sulfidation state and hydrodesulfurization mechanism on Mo/TiO₂ catalyst using ³⁵S radioisoprene tracer methods. Applied Catalysis A: General 224: 191-199.
- Wang, L., and Qing, C. (2011). Pyrolysis [Online], Available from: <http://www.londonenergysaver.ca/PDFs/Uwo/Pyrolysis.pdf>, [2013,June 6].

- Wang, W., Liu, P., Zhang, M., Hu, J., and Xing, F. (2012). The pore structure of phosphoaluminate cement. Open Journal of Composite Materials 2: 104-112.
- Williams, P. T. (2013). Pyrolysis of waste tyres: A review. Waste Management 33: 1714-1728.
- Williams, P. T., and Bottrill, R.P. (1995). Sulfur-polycyclic aromatic hydrocarbons in tyre pyrolysis oil. Fuel 74: 736-742.
- Xiang, C. E., Chai, Y.M., Liu, Y.Q., and Liu, C.G. (2008). Mutual influences of hydrodesulfurization of dibenzothiophene and hydrodenitrogenation of indole over NiMoS/ γ -Al₂O₃ catalyst. Journal of Fuel Chemistry and Technology 36(6): 684-690.
- Yaseen, M., Shakirullah, M., Ahmad, I., Rahman, A.U., Rahman, F.U., Usman, M., and Razzaq, R. (2012). Simultaneous operation of dibenzothiophene hydrodesulfurization and methanol reforming reactions over Pd promoted alumina based catalysts. Journal of Fuel Chemistry and Technology 40(6): 714-720.
- Yoosuk, B., Kim, J.H., Song, C., Ngamcharussrivichai, C., and Prasassarakich, P. (2008). Highly active MoS₂, CoMoS₂ and NiMoS₂ unsupported catalysts prepared by hydrothermal synthesis for hydrodesulfurization of 4,6-dimethyldibenzothiophene. Catalysis Today 130: 14-23.
- Yu, Z., Fareid, L.E., Moljord, K., Blekkan, E.A., Walmsley, J.C., and Chen, D. (2008). Hydrodesulfurization of thiophene on carbon nanofiber supported Co/Ni/Mo catalysts. Applied Catalysis B: Environmental 84: 482-489.
- Zepeda, T. A., Pawelec, B., Fierro, J.L.G., Olivas, A., Fuentes, S., and Halachev, T. (2008). Effect of Al and Ti content in HMS material on the catalytic activity of NiMo and CoMo hydrotreating catalysts in the HDS of DBT. Microporous and Mesoporous Materials 111: 157-170.
- Zhao, H. (2009). Catalytic Hydrogenation and Hydrodesulfurization of Model Compounds [Online], Available from: [http://www.scholar.lib.vt.edu/theses/available/etd-03272009-233526/unrestricted/dissertation 5-5-2009.pdf](http://www.scholar.lib.vt.edu/theses/available/etd-03272009-233526/unrestricted/dissertation%205-5-2009.pdf), [2013, June 27].



APPENDIX

จุฬาลงกรณ์มหาวิทยาลัย
CHULALONGKORN UNIVERSITY

APPENDIX A

CALCULATION OF PRODUCT YIELDS

The total conversion and product yields were calculated by the following expressions:

$$\% \text{ Liquid yield} = 100 \times (W_{\text{Liq}} / W_{\text{Daf}})$$

$$\% \text{ Solid yield} = 100 \times (W_{\text{R}} / W_{\text{Daf}})$$

$$\% \text{ Gas yield} = 100 - \% \text{Liquid yield} - \% \text{Solid yield}$$

where:

W_{Daf} = weight of dry-ash free waste tire

W_{R} = weight of dry-ash free residue remained after THF solvent washing and drying

W_{Liq} = weight of liquid

Example:

Pyrolysis condition:

- Reaction temperature: 400 °C
- Reaction time: 10 min
- N₂ flow rate: 0.1 L/min

Calculation:

Weight of initial waste tire = 100 g

Weight of dry-ash free waste tire = 100.28 g

Weight of pyrolysis condensed oil = 42.12 g

Weight of pyrolysis residual oil = 4.01 g

Weight of liquid = 46.13 g

Weight of dry-residual solid = 41.72

$$\% \text{ Liquid yield} = 100 \times (46.13/100.28) = 46.00$$

$$\% \text{ Solid yield} = 100 \times (41.72/100.28) = 41.60$$

$$\% \text{ Gas yield} = 100 - 46.00 - 41.60 = 12.40$$

APPENDIX B

CALCULATION OF GROSS CALORIFIC HEATING VALUE

Gross calorific heating value of solid was determined following Standard Test Method for Gross Calorific Value of Coal and Coke by Adiabatic Bomb Calorimeter (ASTM D2015)

Summary of Test Method

The heat capacity of the calorimeter is determined by burning a specified mass of benzoic acid in oxygen. A comparable amount of the analysis sample is burned under the conditions in the calorimeter. The calorific value of the analysis sample is computed by multiplying the corrected temperature rise, adjusted for extraneous heat effects, by the heat capacity and dividing by the mass of the sample.

Apparatus

1. Oxygen Bomb calorimeter

Reagents

1. Distilled water
2. Standard benzoic acid available from the National Institute of Standards and Technology (NIST)
3. Oxygen 99.5%
4. Methyl orange
5. Sodium carbonate (Na_2CO_3) (Dissolve 3.57 g of sodium carbonate, dried for 24 h at 105 °C in deionized water, and diluted to 1 L).
6. Water for washing of the bomb interior (1 mL of methyl orange is diluted in 1 L of deionized water).

Determination of the heat capacity of the calorimeter

1. Weight 0.8-1.2 g of benzoic acid into a sample holder. Record sample weight to the nearest 0.0001 g.
2. Connect a measured fuse in accordance with manufacture's guidelines.
3. Rinse the bomb with water to wet internal seals and surface areas of the bomb or precondition the calorimeter according to the manufacture's instructions. Add 1.0 mL of water to the bomb before assembly.

4. Assemble the bomb. Admit oxygen to the bomb to a consistent pressure of between 30 atm. The same pressure is used for each heat capacity run. Control oxygen flow to the bomb so as not to blow material from the sample holder.
5. Fill the calorimeter vessel with water at a temperature not more than 2 °C below room temperature and place the assembled bomb in the calorimeter. Check that no oxygen bubbles are leaking from the bomb.
6. Allow 5 min for the temperature of the calorimeter vessel to stabilize.
7. Fire the charge.
8. For adiabatic calorimeters adjust the jacket temperature to match that of the calorimeter vessel temperature during a period of the rise. Record the first reading after the rate of change has stabilized the final temperature.
9. Open the calorimeter and remove the bomb.

Follow the procedures as described in 1-9 for determination of heat capacity of waste tire and pyrolysis oil. Calculate the gross calorific value using the following equation:

$$Q_v (\text{gross}) = [(TE) - e_1 - e_2 - e_3]/g$$

Where:

Q_v (gross) = gross calorific value at constant volume as determined (J/g)

E = the heat capacity of the calorimeter (J/°C)

T = corrected temperature rise (°C)

e_1 = volume of the titrant (sodium carbonate) (mL)

e_2 = the length of fuse consumed during combustion (cm) × the

heat of

combustion the firing fuse (J/cm)

e_3 = 25×10^3 (J) × wt% sulfur in the sample × mass of sample (g)

g = mass of the sample (g)

APPENDIX C

CALCULATION OF %SULFUR REMOVAL

The influence of catalyst concentration on the degree of hydrodesulfurization of the pyrolysis oil derived from waste tire can be calculated as shown below:

Condition:

- Catalyst concentration: 0 – 2.0 wt %
- Reaction temperature: 250 °C
- Reaction time: 30 min
- Initial hydrogen pressure: 20 bar

%Sulfur removal was calculated using the following equation:

$$X = \left[\frac{C_0 - C_1}{C_0} \right] \times 100$$

Where:

X = %Sulfur removal

C_0 = total area of sulfur content before hydrodesulfurization

C_1 = total area of sulfur content after hydrodesulfurization

CHULALONGKORN UNIVERSITY

Table C-1 The influence of catalyst concentration on degree of hydrodesulfurization

	%catalyst loading (%wt)	C ₀	C ₁	%Sulfur removal
NiMo/ γ-Al ₂ O ₃	0	654315	551190	15.76
	0.1	654315	422194	35.47
	0.3	654315	289506	55.75
	0.5	654315	203383	68.91
	0.7	654315	129608	80.19
	1.0	654315	100514	84.63
	1.5	654315	100532	84.63
	2.0	654315	79933	87.78

%Sulfur removal of pyrolysis oil after hydrodesulfurization for 2.0%wt catalyst loading was calculated as followed:

$$\% \text{Sulfur removal} = \left[\frac{C_0 - C_1}{C_0} \right] \times 100$$

$$\% \text{Sulfur removal} = \left[\frac{654315 - 79933}{654315} \right] \times 100$$

$$= 87.8 \%$$

APPENDIX D
DATA OF SULFUR REMOVAL EFFICIENCY

Table D-1 Influence of catalyst concentration on degree of sulfur removal

	%catalyst loading (%wt)	C ₀	C ₁	%Sulfur removal
Mo/ γ -Al ₂ O ₃	0	654315	551190	15.76
	0.5	654315	469888	28.18
	1.0	654315	421247	35.62
	2.0	654315	324674	50.37
NiMo/ γ -Al ₂ O ₃	0	654315	551190	15.76
	0.1	654315	422194	35.47
	0.3	654315	289506	55.75
	0.5	654315	203383	68.91
	0.7	654315	129608	80.19
	1.0	654315	100514	84.63
	1.5	654315	100532	84.63
	2.0	654315	79933	87.78
CoMo/ γ -Al ₂ O ₃	0	654315	551190	15.76
	0.1	654315	468516	28.39
	0.3	654315	416089	36.40
	0.5	654315	336069	48.63
	0.7	654315	201041	69.27
	1.0	654315	165467	74.71
	1.5	654315	148859	77.24
	2.0	654315	138518	78.83

Table D-2 Influence of initial hydrogen pressure on degree of sulfur removal

	Initial hydrogen pressure (bar)	C ₀	C ₁	%Sulfur removal
Mo/ γ -Al ₂ O ₃	10	654315	423992	35.20
	30	654315	363506	44.44
	50	654315	138464	59.05
NiMo/ γ -Al ₂ O ₃	10	654315	252690	61.38
	20	654315	203383	68.91
	30	654315	166504	74.55
	40	654315	114598	82.48
	50	654315	103004	84.25
CoMo/ γ -Al ₂ O ₃	10	654315	368589	43.66
	20	654315	336069	48.63
	30	654315	163830	74.96
	40	654315	135287	79.32
	50	654315	114598	82.48

Table D-3 Influence of reaction temperature on degree of sulfur removal

	Reaction temperature (°C)	C ₀	C ₁	%Sulfur removal
Mo/ γ -Al ₂ O ₃	150	654315	513664	21.49
	250	654315	389317	40.50
	350	654315	337441	48.42
NiMo/ γ -Al ₂ O ₃	150	654315	429935	34.29
	200	654315	203383	68.91
	250	654315	189402	71.10
	300	654315	154286	76.42
	350	654315	101189	84.53
CoMo/ γ -Al ₂ O ₃	150	654315	479561	26.70
	200	654315	412525	36.95
	250	654315	336069	48.63
	300	654315	187129	71.40
	350	654315	135758	79.25

Table D-4 Influence of reaction time on degree of sulfur removal

	Reaction time (min)	C ₀	C ₁	%Sulfur removal
Mo/ γ -Al ₂ O ₃	5	654315	598819	8.48
	30	654315	557943	14.72
	60	654315	400158	38.84
NiMo/ γ -Al ₂ O ₃	5	654315	254989	61.03
	10	654315	226960	65.31
	20	654315	221478	66.15
	30	654315	203383	68.91
	40	654315	183942	71.88
	50	654315	122213	81.32
	60	654315	109740	83.22
CoMo/ γ -Al ₂ O ₃	5	654315	533750	18.42
	10	654315	466977	28.63
	20	654315	448617	31.44
	30	654315	336069	48.63
	40	654315	284593	56.50
	50	654315	218206	66.65
	60	654315	173483	73.48

VITA

Mr. Nut Jantaraksa was born on June 27, 1988 in Prachinburi, Thailand. He graduated Bachelor's Degree of Engineering in the major of petrochemicals and polymeric materials from Faculty of Engineering and industrial technology, Silpakorn University in 2010. He has been a graduate student studying in the program of Petrochemistry and Polymer Science at Faculty of Science, Chulalongkorn University and finished his study in 2013.

Articles in peer-reviewed conference proceedings

Jantaraksa, N ., Prasassarakich, P ., Hinchiranan, N. (2012). Hydrodesulfurization of oil derived from waste tire pyrolysis. Proceeding of the 10th Eco-Energy and Materials Science and Engineering Symposium, Ubon ratchatani, Thailand, December 5-8 2012.